

2019 GEOPRISMS

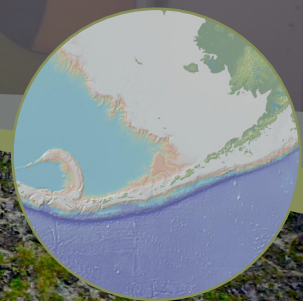
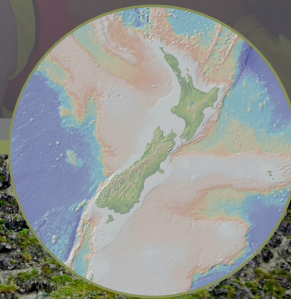
SYNTHESIS & INTEGRATION

THEORETICAL AND EXPERIMENTAL INSTITUTE



ABSTRACT VOLUME

Menger Hotel • San Antonio, TX
February 27-March 1, 2019



Geodynamic Processes at Rifting and Subducting Margins



GeoPRISMS is funded by the National Science Foundation

The GeoPRISMS Office
The Pennsylvania State University
Department of Geosciences
503 Deike Building
University Park, PA 16802-2714
info@geoprisms.org

www.geoprisms.org



Top | Deployment of an ocean bottom seismometer during the Hikurangi Ocean Bottom Investigation of Tremor and Slow Slip (HOBITSS) experiment. Photo credit: Takeo Yagi
Bottom | Pacific coast outcrops on Unalaska Island, eastern Aleutians. The rocks in the lower outcrop behind Merry are pillow lavas. The mottled appearance is produced by the reddish-brown pillow interiors, surrounded by green, inter-pillow sediment and altered pillow rinds. The upper part of the outcrop is an andesite sill with short, columnar joints at 90° to the horizontal contact. These rocks were formed prior to affects of crustal thickening by magmatism and accretionary tectonics, which eventually lead to the emergence of the large islands that we see in the eastern Aleutians today. Photo credit: Gene Yogodzinski
Maps generated using GeoMapApp.

Poster list

Theme A: Deformation at all time scales

Theme B: Mass fluxes

Presenter		ID	Poster title	Page
Abers	Geoff	A 99	<i>AACSE: The Alaska Amphibious Community Seismic Experiment</i>	9
Andrys	Janine	B 1	<i>Volatile contents of Western Aleutian magmas and their relationship to slab thermal structure</i>	70
Beaudoin	Grace	B 2	<i>From AOC to eclogite: Halogen behavior during devolatilization in the forearc</i>	71
Bécel	Anne	A 36	<i>New constraints on the final stages of breakup and early spreading history of the Eastern North American Margin from MCS data of the Community Seismic Experiment</i>	10
Belzer	Benjamin	A 37	<i>Constitutive behavior of chlorite-rich fault gouge under hydrothermal conditions</i>	11
Biemiller	James	A 38	<i>Short- and long-term deformation styles on an active low-angle normal fault: Mai'iu fault, Papua New Guinea</i>	12
Blank	David	A 39	<i>Precursory stress changes and fault dilation lead to fault rupture: Insights from Discrete Element Simulations</i>	13
Bodmer	Miles	A 40	<i>Does subslab buoyancy govern segmentation of Cascadia's forearc topography?</i>	14
Buck	W. Roger	A 41	<i>Preliminary attempts to relate seismic coupling of shallow megathrusts to upper plate extension through changes in pore pressure</i>	14
Carbotte	Suzanne	A 42	<i>Plans for a new long-offset multi-channel seismic experiment of the Cascadia Subduction Zone in summer 2020</i>	16
Carchedi	Christopher	A 43	<i>Investigating short-period microseisms near Lake Malawi using a broadband array of onshore and lake-bottom seismometers</i>	17
Chiasera	Brandon	B 3	<i>Geochemically constraining the depth of the lithosphere-asthenosphere boundary in the Central Main Ethiopian Rift System</i>	72
Conder	James	A 44	<i>Numerical modeling of great earthquakes on the seismogenic zone</i>	18
de Sagazan	Clément	A 45	<i>Feedbacks between sedimentation, normal faulting, and magmatic accretion at the Andaman Sea spreading center</i>	19
DeBari	Susan	B 4	<i>Building arc crust – plutonic to volcanic connections in an extensional oceanic arc, the Alisitos arc crustal section (southern Rosario segment), Baja California</i>	73
DeBari	Susan	B 100	<i>Recontextualization of across-arc signatures in the Izu Bonin arc, linking mafic to felsic magmatism across the arc</i>	74
Delph	Jonathan	B 5	<i>Insights into the architecture of active continental arcs from geochemical and seismic data</i>	75
Droof	Connor	A 46	<i>New constraints on volcanic inflation and trench behavior around Mt. Veniaminof, Alaska from GPS campaign measurements</i>	20

Presenter		ID	Poster title	Page
Ducatte	Alexandra	B 6	<i>Evaluating the origin of pyroxenite xenoliths in the East African Rift System via Re-Os isotopes and highly-siderophile elements</i>	76
Dufek	Josef	B 7	<i>Using magma dynamics models to integrate geochemical and geophysical data in a process-based framework</i>	77
Ebinger	Cynthia	A 47	<i>Geometry and kinematics of active faults in the magma-poor Malawi rift, East Africa</i>	21
Eilon	Zachary	B 8	<i>New constraints on the East African rift from axis to flank using a combination of seismic data types</i>	78
Emishaw	Lulseged	A 48	<i>Depth and time dependence of strain partitioning in the development of late Jurassic – early Paleogene and Neogene - Quaternary extensional structures within the Turkana depression, East Africa</i>	22
Emry	Erica	A 49	<i>Upper mantle structure beneath the East African Rift System from full-wave ambient noise tomography</i>	23
Estep	Justin	B 9	<i>Seismic layer 2A: Evolution and thickness from 0-70 Ma crust in the slow-intermediate spreading South Atlantic</i>	79
Fliedner	Céline	A 50	<i>Seismic wave propagation in Orocopia schist</i>	24
Gaherty	James	A 52	<i>Presence and role of partial melt in continental rifting</i>	25
Gase	Andrew	A 53	<i>Crustal structure of the northern Hikurangi margin from marine seismic reflection imaging and onshore-offshore seismic tomography: implications for megathrust heterogeneity and overpressure in a region of shallow slow earthquakes</i>	26
Gulick	Sean	A 55	<i>From rifting to subduction: Subduction initiation at the Puysegur Trench, New Zealand</i>	27
Ha	Goeun	B 10	<i>Effect of thermally-controlled permeability barriers on the location of arc volcanism at subduction zones</i>	80
Han	Shuoshuo	A 56	<i>3D seismic images of double BSRs at the northern Hikurangi margin and the implications for subduction processes</i>	28
Harris	Robert	A 57	<i>Variations in the apparent coefficient of friction, Hikurangi margin, New Zealand</i>	29
Harvey	Kayleigh	A 60	<i>Hot slab time machine: Petrochronologic evidence for protracted amphibolite-facies metamorphism of the Catalina Schist (Santa Catalina Island, CA)</i>	30
Haynie	Kirstie	A 58	<i>Revisiting the 1964 Great Alaska Earthquake in a slab-driven forearc Sliver-escape tectonics framework</i>	31
Hightower	Erin	A 59	<i>Gravitational modeling of crustal structure and composition of the Puysegur Margin, South Island, New Zealand: Insights into subduction initiation</i>	32
Hoggard	Mark	B 11	<i>Billion-year stability of cratonic edges controls location of global sediment-hosted metals</i>	81
Hole	John	A 61	<i>The effects of thick sediment upon continental breakup: Kinematic and thermal modeling of the Salton Trough, southern California</i>	33
Hoover	William	B 12	<i>Low-salinity fluids in an intra-slab shear zone: Insights into fluid salinity from apatite in the Monviso Ophiolite (Western Alps)</i>	82
Hyndman	Roy	A 62	<i>Slow slip and tremor: A review of the role of water expelled from subducting plate</i>	34

Presenter		ID	Poster title	Page
Ide	Satoshi	A 63	<i>Slow earthquakes worldwide: Database and interpretation with the science of Slow Earthquakes Project</i>	35
Ishimwe	Felix	B 13	<i>Potential causes of crystal-melt disequilibrium in Karisimbi lava</i>	83
Ito	Garrett	A 64	<i>Width of imbricated thrust blocks and the strength of accreting sediments at submarine wedges</i>	36
Jammes	Suzon	A 65	<i>Effect of contrasting strength from inherited crustal fabric on the development of rifting margins: The example of the Northeastern Canadian margin</i>	37
Janiszewski	Helen	A 66	<i>Receiver function imaging of magmatic- and subduction-related structures beneath arc volcanoes: A case study at Cleveland Volcano, Alaska</i>	38
Jeppson	Tamara	A 67	<i>Lithology and cement controls on the evolution of compressional wave velocity and porosity in input materials at northern Sumatra and other subduction zones</i>	39
Jones	Meghan	B 14	<i>Pyroclast transport dynamics during the 2012 eruption of Havre Volcano (Kermadec Arc)</i>	84
Kardell	Dominik	B 15	<i>Structure of upper oceanic crust in the western South Atlantic using full-waveform velocity modeling</i>	85
Kent	Adam	B 16	<i>The initiation of volcanic eruptions</i>	86
Kenyon	Lindsey	A 68	<i>Implications of subduction obliquity to the inferences of seismic anisotropy in the mantle wedge</i>	40
Kotowski	Alissa	A 69	<i>Preliminary petrologic and microstructural characterization of a metamorphic section beneath the Samail (Oman) Ophiolite: Results from the Oman Drilling Project Hole BT1B</i>	41
Kuo	Szu-Ting	A 70	<i>Experimental constraints on mechanical behaviors of the inner accretionary prism sediments at the Nankai subduction zone</i>	42
Laó-Dávila	Daniel	A 71	<i>The IRES Malawi Rift Project: Synthesis and future directions</i>	43
Liu	Yiduo	A 72	<i>The second half of plate tectonics: 3-D mapping of the remnant "Paleo-Pacific" slabs in the lower mantle under East Asia and its tectonic implications</i>	44
Long	Maureen	A 73	<i>Structure, dynamics, and evolution of the Eastern North American Margin: Results from the MAGIC project, Central Appalachians</i>	45
Lubbers	Jordan	A 74	<i>Diffusion chronometry in sanidine: Helping unravel thermal histories of large silicic magma reservoirs</i>	46
Lynner	Colton	A 75	<i>Tilt and compliance corrections for the ENAM broadband OBS instruments</i>	47
Magni	Valentina	A 76	<i>The effects of back-arc spreading on arc magmatism</i>	48
Martinez	Fernando	A 77	<i>Northern Lau Basin tectonics and volcanism along a propagating slab tear</i>	49
Monteleone	Vanessa	A 78	<i>Rifting evolution of the Eastern Black Sea Basin from long-offset seismic reflection data</i>	50
Muirhead	James	B 17	<i>How does diffuse CO₂ flux vary across the East African Rift System?</i>	87

Presenter	ID	Poster title	Page
Muth Michelle	B 18	<i>The role of slab melts in the sulfur content, metal content, and oxidation state of primitive arc magmas in the Southern Cascades</i>	88
Newman Andrew	A 79	<i>Completing the megathrust cycle</i>	51
Obana Koichiro	A 80	<i>Seismicity and seismic velocity structure around the trench axis and outer rise region along the Japan Trench</i>	52
Oliva Sarah Jaye	A 98	<i>Insights into fault-magma interactions in an early-stage continental rift from source mechanisms and correlated volcano-tectonic earthquakes</i>	53
Olsen Kelly	A 81	<i>Heterogeneous upper plate extension in South Central Chile and implications for megathrust fault development</i>	54
Oryan Bar	A 82	<i>How shallowing slab dip could produce extensional upper plate earthquakes after a megathrust earthquake?</i>	55
Owens Mary Grace	B 19	<i>Magma and volatile composition of South Island, Turkana</i>	89
Parnell-Turner Ross	B 23	<i>Crustal formation and plume pulsing in the North Atlantic Ocean</i>	90
Peterson Liam	B 20	<i>Crossing the gap: Linking the Eocene and Oligocene East African Rift Volcanics</i>	91
Phillips Rayn	B 21	<i>Spatial distribution of the Amaro and Gamo basalts: Geochemical analysis of the rocks of the Omo River Project</i>	92
Pu Xiaofei	B 22	<i>New olivine-melt Ni thermometer for hydrous basalts and its application to reveal variations in lithospheric thickness in Western Mexico</i>	93
Russell Joshua	A 83	<i>Surface-wave anisotropy of the Eastern North American Margin (ENAM)</i>	56
Sas May	B 24	<i>$\delta^{18}\text{O}$ records in quartz from Okataina volcano, New Zealand: Insights into the evolution of a large and dynamic silicic system</i>	94
Savage Brian	A 84	<i>Body and surface wave tomography of Eastern North American</i>	57
Schlieder Tyler	B 25	<i>Quantifying magma storage timescales and thermal histories for the ~25 ka Oruanui and 1.8 ka Taupo eruptions of the Taupo Volcanic Center, New Zealand</i>	95
Scholl David	A 85	<i>IODP drilling to test end-member ideas about the origin of the Aleutian subduction zone and backarc Bering Sea Region</i>	58
Schwartz Darin	B 26	<i>Upper mantle heterogeneity: Depleted source signature preserved in melt inclusions at coaxial segment of the Juan de Fuca Ridge</i>	96
Shephard Grace	A 86	<i>Plate tectonics and mantle structure of the Arctic, North Atlantic and Panthalassa: Recent updates.</i>	59
Shillington Donna	A 87	<i>Seismic imaging of variations in extension with depth and along-strike in the magma-poor Malawi Rift</i>	60
Shuck Brandon	A 88	<i>The role of mantle melts in the protracted breakup of Pangea</i>	61
Sim Shi Joyce	B 101	<i>A focus on melt focusing</i>	97
Smye Andrew	A 89	<i>Episodic heating of continental lower crust during rifting</i>	62

Presenter		ID	Poster title	Page
Stamps	D. Sarah	A 90	<i>Towards quantifying plume-lithosphere interactions from GNSS geodesy, seismology, and geodynamic modeling</i>	63
Steiner	R. Alex	B 27	<i>Rupturing paradigms of continental rift magmatism: A chemo-spatial analysis of rift magmas</i>	98
Straub	Susanne	B 97	<i>A global view on arc-trench connectivity and andesite petrogenesis</i>	99
Sun	Tianhaozhe	A 91	<i>Studying the coupling between deformation, pore pressure, and fluid flow in subduction forearcs</i>	64
Svoboda	Christopher	B 28	<i>Evolution of transcrustal distillation columns: Evidence from andesites of the Taupo Volcanic Zone</i>	100
Tian	Xiaochuan	B 29	<i>Lithospheric thickness of volcanic rifting margins: Constraints from seaward dipping reflectors</i>	101
Till	Christy	B 30	<i>A model for the first order controls on volcanic repose time</i>	102
Tilley	Hannah	A 92	<i>Along-strike variations in protothrust zone characteristics at the Nankai Trough subduction margin</i>	65
Tobin	Harold	A 93	<i>The SZ4D Vision: Planning for an integrated subduction research program</i>	66
van Dam	Loes	B 31	<i>Material transport in the mantle through 4-D geodynamical models of mid-ocean ridges</i>	108
van Wijk	Jolante	A 94	<i>From source to sink: Tectonic-landscape evolution modeling of a continental rift</i>	67
Wei	S. Shawn	B 32	<i>Seismic constraints on subducted hydrous minerals in the Tonga slab</i>	104
Wiens	Doug	B 33	<i>Mariana subduction zone water input estimated from broadband ocean-bottom seismic data</i>	105
Willis	David	A 95	<i>Neogene stress rotation at the transition from subduction to continental collision, Marlborough, New Zealand</i>	68
Wurth	Kimberly	B 34	<i>Clinopyroxene trace element chemistry as a proxy for magma compositional variations in the Izu Bonin rear arc over the last 14 million years</i>	106
Yang	Xiaotao	B 35	<i>Seismic imaging of slab segmentation and its correlation with volcano distribution along the Aleutian-Alaska subduction zone</i>	107

THEME A | DEFORMATION AT ALL TIME SCALES

Continuous Global Positioning System station installed on the Natron Rift of the East African Rift in Tanzania. The active volcano Ol Doinyo Lengai towers in the background. This GPS station was installed in June 2016. Photo credit: D. Sarah Stamps



AACSE: THE ALASKA AMPHIBIOUS COMMUNITY SEISMIC EXPERIMENT

Abers G., A.N. Adams, P.J. Haeussler, E.Roland, P.J. Shore, D.A. Wiens, S.Y. Schwartz, A.F. Sheehan, D.J. Shillington, S. Webb, L.L. Worthington

The Alaska Amphibious Community Seismic Experiment (AACSE) represents one of the first shoreline-crossing seismic arrays of its kind focused on a subduction zone with prolific earthquake behavior and a complex volcanic arc. The 105 seismic instruments associated with the AACSE are currently deployed along the Alaska Peninsula for a period of approximately 15 months, beginning in Spring 2018. This comprises an array that extends from east of Kodiak Island through the Shumagin Islands, and from the backarc, to more than 200 km outboard of the trench. The AACSE array is complemented by more than a dozen TA and Alaska network stations on land. This effort represents an unprecedented deployment of seismic sensors over the seismogenic zone, sampling a region that spans a hypothesized change in interseismic coupling along the subduction plate boundary, as well as a systematic change in chemical compositions of arc volcanoes. Better understanding structure and seismic behavior across these kinds of transitional boundaries helped to motivate this community effort, and should be made possible by analysis efforts currently being planned across the seismic community using this open-access data. Here we will provide an overview of the current state of the AACSE following the land and ocean-bottom instrument deployments, and servicing of land stations. We will summarize instrument performance across the land portion of the array, including noise levels and data return-rates, and also provide some initial assessments of recorded seismicity rates. Many complementary and add-on experiments have been coordinated in the final year of the experiment, and we will also provide an update on those opportunities and forthcoming datasets.

NEW CONSTRAINTS ON THE FINAL STAGES OF BREAKUP AND EARLY SPREADING HISTORY OF THE EASTERN NORTH AMERICAN MARGIN FROM MCS DATA OF THE COMMUNITY SEISMIC EXPERIMENT

Bécel A., B. Davis, J. Gibson, B. Shuck, H. Van Avendonk

In September-October 2014, the East North American Margin Community Seismic Experiment acquired deep penetration multichannel seismic (MCS) reflection across the Mid-Atlantic continental margin offshore North Carolina. This margin formed after the Mesozoic breakup of supercontinent Pangea. One of the goals of this experiment is an improved understanding of events surrounding final stage of breakup including the relationship between the timing of rifting and the occurrence of offshore magmatism and early spreading history of this passive margin that remain poorly understood. Here we present results from MCS data along two offshore margin normal profiles, spanning from continental crust ~50 km off the coast to mature oceanic crust and a MCS profile along the enigmatic Blake Spur Magnetic Anomaly (BSMA). Initial images reveal a major change in the basement roughness, including a basement step at the BSMA on both margin normal profiles. Seaward of this anomaly, the basement the basement is very smooth and reflective and clear Moho reflections are observed 2.5-3s twt beneath the basement top. Landward of the BSMA, basement is very rough and more typical of very-slow to slow spreading oceanic crust. Differences in basement roughness, internal structures and thickness at BSMA time provide a new view on the formation of this margin.

CONSTITUTIVE BEHAVIOR OF CHLORITE-RICH FAULT GOUGE UNDER HYDROTHERMAL CONDITIONS

Belzer B., M. French

Exhumed and shallowly drilled Mg rich rocks from subduction zones commonly host chlorite which may impact the strength and stability of fault zones. However, the rheology of chlorite at geologically appropriate strain rates, temperatures, and pore pressures has not been systematically studied to determine whether and how chlorite may affect the style of fault slip. To investigate the constitutive behavior of chlorite and the mechanisms controlling its deformation, we present an experimental study on chlorite gouge deformed in general shear. We conducted rate-stepping experiments on 5 mm thick layers of chlorite-rich gouge at 100°C, effective normal stresses of 10 MPa and 70 MPa, pore pressures from 10 MPa to 120 MPa, sliding velocities from 0.001 to 10 $\mu\text{m/s}$, and shear displacements to 6 mm. We observe that the rheological response of chlorite is frictional ($\mu = 0.4\text{-}0.5$) at these conditions, and that higher pore pressure promotes greater frictional strength and rate-strengthening behavior. We also find the velocity dependence of friction transitions between rate-strengthening and rate-weakening at slow slip strain rates. Our results suggest that the rheology of chlorite and mechanisms involving changes in pore volume may be important in controlling slip behavior along faults.

SHORT- AND LONG-TERM DEFORMATION STYLES ON AN ACTIVE LOW-ANGLE NORMAL FAULT: MAI'IU FAULT, PAPUA NEW GUINEA

Biemiller J., L. Wallace, S. Ellis, T. Little, M. Mizera, L. Lavier, S. Webber, F. Taylor, C. Chen, Y. Chou

We compare multi-timescale (years to millions of years) geodetic and geological records of slip on the Mai'iu fault in Southeastern Papua New Guinea, arguably the world's fastest-slipping (~8-12 mm/yr) active low-angle normal fault (LANF) to investigate both the seismic cycle and long-term evolution of LANF detachment systems.

LANFs, which slip at dips of $<30^\circ$, are perplexing because classical fault mechanics predict that normal faults rotated to such low angles should frictionally lock up and that deformation should transition onto newly initiated high-angle normal faults. LANFs are abundant in the geologic record of rifting and often bound metamorphic core complexes; however, actively slipping LANFs are less common and more difficult to identify, in part due to their low slip rates of typically only a few mm/yr.

We present preliminary campaign GPS velocities from a dense network (3-4 km station spacing) across the Mai'iu fault in southeastern New Guinea, which suggest that shallow aseismic creep accommodates a large component of the fault displacement. In contrast, exposed pseudotachylites in exhumed Mai'iu fault zone rocks suggest that the fault is (or once was) seismogenic. These observations may indicate mixed-mode brittle-viscous deformation: the fault creeps over large regions, but also undergoes spatially heterogeneous and temporally transient locking in specific depth ranges. Alternatively, the slip style may have changed over the several Myr duration over which the fault has evolved. We use rate-and-state frictional models to test these scenarios and to model the effects of progressive back-rotation and shallowing of normal faults on their seismic style.

PRECURSORY STRESS CHANGES AND FAULT DILATION LEAD TO FAULT RUPTURE: INSIGHTS FROM DISCRETE ELEMENT SIMULATIONS

Blank D., J. Morgan

We use the discrete element method to create numerical analogs to subduction megathrusts with natural roughness and heterogeneous fault friction. Boundary conditions simulate tectonic loading, inducing fault slip. Intermittently, slip develops into complex rupture events that include foreshocks, mainshocks, and aftershocks. We probe the kinematics and stress evolution of the fault zone to gain insight into the physical processes that govern these phenomena. Prolonged, localized differential stress drops precede dynamic failure, a phenomenon we attribute to the gradual unlocking of contacts as the fault dilates prior to rupture. Slip stability in our system appears to be governed primarily by geometrical phenomena, which allow both slow and fast slip to take place at the same areas along the fault. Similarities in slip behavior between simulated faults and real subduction zones affirm that modeled physical processes are also at work in nature.

DOES SUBSLAB BUOYANCY GOVERN SEGMENTATION OF CASCADIA'S FOREARC TOPOGRAPHY?

Bodmer M., D.R. Toomey, J.J. Roering, L. Karlstrom

Cascadia's forearc topography varies systematically along-strike. This topographic variability reflects long-term patterns of surface uplift and erosion, however, the underlying drivers of uplift and the mechanisms supporting present day topography are unclear. Here, we synthesize results from seismic imaging, observations of vertical deformation, and characteristics of the megathrust interface to infer that buoyancy in the subslab asthenosphere influences the development and stability of Cascadia forearc topography. The northern and southern segments of Cascadia are characterized by rapid short- and long-term uplift rates, rapid erosion rates, shallower slab dip angles, and increased plate locking compared to the central segment. Similarly, tomographic images show segmented low-velocity anomalies beneath northern and southern Cascadia. These low-velocity anomalies reflect localized upwellings and regions of excess buoyancy. We propose that buoyant regions influence the integrated shear force at the megathrust by either shallowing slab dip or increasing the strength of the megathrust. Either scenario locally increases the integrated shear force, which has implications for long-term topographic development and the force balance sustaining high elevations. Because interseismic uplift, long-term uplift and erosion, and topography exhibit similar increases north and south, we infer that unrecovered interseismic strain leads to long-term deformation. Using inferred values for slab dip and plate coupling we predict first-order variations in forearc topography. Our analysis suggests that lateral support for topography in Cascadia may be due to variations in the net shear force at the megathrust interface. Variations in subslab buoyancy may be critical to explaining forearc highs in this and other subduction systems.

PRELIMINARY ATTEMPTS TO RELATE SEISMIC COUPLING OF SHALLOW MEGATHRUSTS TO UPPER PLATE EXTENSION THROUGH CHANGES IN PORE PRESSURE

Buck W.R., B. Oryan

Unprecedented data sets collected before, during and after the Tohoku Earthquake of March 11, 2011 showed that up to 70 meters of slip occurred on the shallowest part of the subduction interface during that event. This “slip-to-the-trench” was also implicated in the extreme height of the resulting tsunami. This shallow slip was not expected for several reasons including that the weak, overpressured sediments of the accretionary prism should not be strong enough to maintain significant shear stresses. Post-seismic extension of the upper plate was indicated by aftershock studies, since most of the nearly 2000 upper plate aftershocks were extensional and located between ~30 and 230 km from the trench and going down to depth of 30 km. Since the Tohoku Earthquake, evidence has been compiled showing an association of extensional upper plate aftershocks and tsunamicgenic megathrust earthquakes (i.e. earthquakes producing much larger-than-expected tsunami for the size of the earthquake). In a recent study we developed numerical models showing that reduction of the dip of a subducting slab on a geologic time scale could produce an extensional stress state in the plate above the interface. Here we discuss numerical models designed to investigate whether upper plate extension could reduce pore pressure in an accretionary wedge. Specifically, we assume that pore pressure changes relate to changes on total pressure. Extensional strain implies a reduction in horizontal stress and so total pressure and this may increase the coupling with the downgoing plate.

PLANS FOR A NEW LONG-OFFSET MULTI-CHANNEL SEISMIC EXPERIMENT OF THE CASCADIA SUBDUCTION ZONE IN SUMMER 2020

Carbotte S., J.P. Canales, S. Han, A. Calvert, M. Nedimovic, C. Goldfinger, H. Tobin, A. Trehu

In this presentation plans for a new regional-scale long-offset multi-channel seismic study of the Cascadia subduction zone to be conducted in summer 2020 will be presented. The survey will span the full length of the subduction zone and is designed to investigate how the geologic structure and properties of this subduction zone vary both along and across the margin. Our study will use ultra-long-offset multi-channel seismic (MCS) data to characterize subducting plate and accretionary wedge structure, and properties of the megathrust, to address the following specific questions: 1. Are there any systematics in the structure and properties of the incoming Juan de Fuca plate, the megathrust zone, and accretionary wedge associated with inferred paleo-rupture segmentation? 2. Are there down-dip variations in megathrust geometry and reflectivity indicative of transitions in fault properties, and what are the properties of the potentially tsunamigenic shallow portion of the megathrust? Long 15-km-offset MCS data will be acquired along twenty 2-D profiles at 50-100 km spacing oriented perpendicular to the margin and located to provide coverage in areas inferred to be paleo-rupture patches and their boundary zones. The survey will also include one continuous strike line along the continental shelf centered roughly over gravity-inferred fore-arc basins to investigate possible segmentation near the down-dip limit of the seismogenic zone. The data will be made available to the community, providing a high-quality data set illuminating the regional subsurface architecture all along the Cascadia Subduction Zone.

INVESTIGATING SHORT-PERIOD MICROSEISMS NEAR LAKE MALAWI USING A BROADBAND ARRAY OF ONSHORE AND LAKE-BOTTOM SEISMOMETERS

Carchedi C., J. Gaherty, D. Shillington, N. Accardo, C. Scholz, P. Chindandali, R. Ferdinand, A. Nyblade

Newly-available broadband seismic data surrounding Lake Malawi provide an opportunity to investigate interactions between lake processes and the ambient seismic noise field. Recent studies near lakes identify pervasive noise signals between periods of 0.5 and 5 s which are observable as far as 300 km away from the interpreted lacustrine source, but the precise physical mechanism producing these signals remains unclear. The SEGMeNT (Study of Extension and maGmatism in Malawi aNd Tanzania) experiment included the deployment of fifty-seven onshore broadband seismometers and six broadband lake-bottom seismometers (LBS) in water depths between 270 and 680 m in Lake Malawi. Lake Malawi covers nearly 30,000 km² of the southern East African Rift and by volume is the fifth largest lake in the world. This project provides one of the only broadband seismic datasets collected in a sublacustrine environment.

Power spectral analyses at stations surrounding and within Lake Malawi reveal a transient noise signal that manifests daily as swells in power that persist for several hours and peak near 1-3 s - a signature distinct from those of ocean microseisms. Onshore, the signals are strongest close to the lake and decay with distance from the shoreline. Offshore, the signals extend to slightly longer period (1-5 s). In both cases, signal amplitude is highest during the local overnight hours. Preliminary application of frequency-dependent polarization analysis suggests that the onshore signals are Rayleigh-waves consistent with a source near the northern lake shoreline, while the lake-bottom signals align with the direction of maximum fetch.

NUMERICAL MODELING OF GREAT EARTHQUAKES ON THE SEISMOGENIC ZONE

Conder J., A. Butler

Some subduction zones are more prone to great earthquakes than others. Why this is so may have to do with factors including width of the seismogenic zone and/or smoothness of the megathrust. To test the sensitivity of great earthquake production to these parameters, we develop a finite difference model of slip on a fault zone consisting of three layers of nodes that track elastic stress and strain with systematic tectonic movement. Slip occurs on the middle layer when critical stress at a location is reached, often causing a local failure cascade defining an individual seismic event. The model retains strain history to follow the system through multiple seismic cycles. Restricting the downdip limit reduces the frequency of the largest events as there are fewer pathways to exploit a continuing cascade along-strike. Variable friction also impacts the frequency of the largest events. Sticky patches inhibit large ruptures from occurring along the length of the seismogenic zone, often rupturing somewhat independently from the rest of the system. Slippery patches are more complex. While they often inhibit large ruptures by releasing stress in small events, if a slippery patch is close to critical during rupture of other nodes in the region, the patch may instead facilitate a larger rupture than would have otherwise occurred. This behavior of low-friction patches usually inhibiting, but occasionally facilitating rupture explains how seamounts and other asperities sometimes seem to behave in contradictory ways even in the same subduction system.

FEEDBACKS BETWEEN SEDIMENTATION, NORMAL FAULTING, AND MAGMATIC ACCRETION AT THE ANDAMAN SEA SPREADING CENTER

de Sagazan C., J-A. Olive

We investigate the impact of sedimentation on the dynamics of seafloor spreading along the Andaman Sea spreading center (ASSC, full spreading rate: 3.8 cm/yr), in the back-arc domain of the Sumatra subduction zone. This spreading segment displays features similar to those of an intermediate / slow-spreading mid-ocean ridge, e.g., an axial valley bounded by axis-facing normal faults and seismically-inferred axial melt lenses. It is however overlain by a ~2-km thick layer of terrigenous sediments. Further, crustal-scale normal faults have recently been imaged at the ASSC, and show unusually shallow dips (~30°) and large spacing (> 10 km) compared to those found at mid-ocean ridges of commensurate spreading rate.

To assess whether these unusual tectonic characteristics can be directly attributed to sediment deposition, we incorporate sedimentation in 2-D numerical models of seafloor spreading. In these models, a fraction M of the imposed extensional strain is accommodated by on-axis magmatic injection. Sediment deposition is simulated by adding mass on top of the model domain at a constant rate, and rapidly diffusing the resulting topography to obtain a flat seafloor. Accounting for sedimentation drastically increases fault lifespan and characteristic spacing (up to a factor of ~2) for a given M . Longer fault lifespan enables greater amounts of rotation, from ~60° to ~30°, as observed at the ASSC. We argue that the primary effect of sedimentation is to reduce the energy cost associated with normal fault growth, which promotes sustained strain localization.

NEW CONSTRAINTS ON VOLCANIC INFLATION AND TRENCH BEHAVIOR AROUND MT. VENIAMINOF, ALASKA FROM GPS CAMPAIGN MEASUREMENTS

Droof C., J. Freymueller, S. Li

Volcanic inflation is often the result of multiple processes operating on a variety of different timescales. Such is the case at Mt. Veniaminof, located in the central Alaska Peninsula. The volcano is relatively poorly instrumented, owing to its remote location and the presence of a glacier-filled summit caldera. The extent of GPS measurements on the direct volcanic edifice is limited to 3 campaign surveys conducted in 2002, 2005, and 2017. In this study, we use the 2017 campaign measurements along with the slab2.0 subduction interface geometry in order to refine the locking model of the Shumagin segment of the Aleutian trench and better predict the tectonic component of geodetic signal on the volcano. We then use the residual velocities to model volcanic inflation, which is shown to cause average horizontal surface displacements of 1 - 2.5 mm/yr on the direct volcanic edifice. We then subtract the inflationary signal from our initial velocities in order to obtain an improved trench locking model and better characterize slip behavior. We show that repeated iteration of this process extends trench locking further down dip and that discrete along-strike boundaries over which trench locking changes likely display subtle, short wavelength variations.

GEOMETRY AND KINEMATICS OF ACTIVE FAULTS IN THE MAGMA-POOR MALAWI RIFT, EAST AFRICA

Ebinger C., S.J. Oliva, TQH Pham, S. Henderson, K. Peterson, P. Chindandali, R. Gallacher, F. Illsley-Kemp, N. Accardo, G. Mulibo, R. Wambura-Ferdinand, G. Mbogoni, D. Shillington, J. Gaherty, A. Nyblade

Continental rift zones show a regular along-axis segmentation into half-graben basins, but the distribution of strain between border and intrabasinal faults during rift evolution and role of magmatism remain debated. Does magma intrusion accommodate significant strain outside isolated magmatic provinces? Has strain migrated from border faults to intrabasinal faults?

Earthquake distributions and source mechanisms from the active N Malawi rift and Miocene-Recent Rungwe volcanic province provide constraints on fault kinematics and crustal rheology during rifting of cratonic lithosphere. North basin was the site of damaging earthquakes in 2009.

DEPTH AND TIME DEPENDENCE OF STRAIN PARTITIONING IN THE DEVELOPMENT OF LATE JURASSIC – EARLY PALEOGENE AND NEOGENE - QUATERNARY EXTENSIONAL STRUCTURES WITHIN THE TURKANA DEPRESSION, EAST AFRICA

Emishaw L., M.G. Abdelsalam

The Turkana Depression (TD) is a NW-trending topographic corridor within the East African Rift System (EARS). It is bounded by the Ethiopia-Yemen plateau and the East Africa plateau. The depression is dominated by Precambrian basement rocks, Mesozoic and Cenozoic rift sediment, and Cenozoic volcanic rocks. The Anza rift is a NW-trending failed arm of a late Jurassic triple junction. The Anza rift is intersected by the N-trending segments of the EARS including the Kino Sogo and Turkana rifts. We imaged crustal and lithospheric thickness beneath the TD using satellite gravity data. We also used these data to model upper crustal density distribution of the Kino Sogo rift and the underlying Anza rift. Our results show thinner crust (between 24 and 28 km) and lithosphere (between 150 and 120 km) beneath the TD. Our results also show that the crust is dominated by broad NW-trending density anomalies between 5 and 10 km depth. Differently, narrow N-trending density anomalies dominate the upper crust between 0 and 5 km depth. We propose that the dominant deeper NW-trending crustal structure beneath the TD is associated with the Anza rift whereas some segments of the EARS are expressed only at the shallow crustal depth.

UPPER MANTLE STRUCTURE BENEATH THE EAST AFRICAN RIFT SYSTEM FROM FULL-WAVE AMBIENT NOISE TOMOGRAPHY

Emry E., Y. Shen, A. Nyblade, A. Flinders, X. Bao

The relationship between mantle dynamics, lithospheric structure, and rift development along the East African Rift System (EARS) has been hindered by uneven seismic instrumentation, producing well-resolved structure beneath some rift segments, but lacking resolution along other segments and adjacent regions. To address this, we used a long-period ambient noise full waveform tomography approach on data from 186 broadband seismic stations throughout Africa and surrounding regions to image upper mantle structure in Africa. We used a frequency-time normalization method to extract empirical Green's functions (EGFs) from ambient seismic noise and used a finite-difference waveform inversion to iteratively invert fundamental mode Rayleigh waves from the EGFs, using periods of 40-340 seconds. The results provide isotropic, shear-velocity for the upper mantle beneath Africa. Key results include extremely low shear velocities in the upper mantle beneath the highly magmatic northern and eastern sections of the EARS, which are separate at mid-upper mantle depths and extend to the mantle transition zone. High shear-velocity dominates in the southern and western EARS at the uppermost mantle, with distinct, low-velocity anomalies mostly beneath regions of current volcanism; at deeper upper mantle depths, the pattern switches to low-velocities. We also image discontinuously low-velocity structure at shallow and deep upper mantle beneath Turkana, low-velocity features at mid-upper mantle depths beneath a part of the southwestern EARS, and high-velocity upper mantle beneath the southern Malawi rift. We interpret the patterns as a set of secondary upwellings from mantle transition zone that are diverted by lithospheric structures towards regions of thinner lithosphere.

SEISMIC WAVE PROPAGATION IN OROCOPIA SCHIST

Flidner C., M. French

In subduction zones, seismic tomography shows regions of high V_p/V_s , inferred to be evidence of high fluid pressure, in regions of slow fault slip. In other cases, high fluid pressure is proposed to preferentially attenuate the high-frequency seismic waves generated by fault slip, thereby limiting our ability to constrain the underlying physics. However, quantifying these effects is challenging because the dynamic elastic moduli and anelastic properties of subduction zone rocks are poorly constrained. We are measuring the ultrasonic velocities and frequency-dependent attenuation of elastic waves in the Orocopia schist as a function of pressure and temperature. Experiments to measure ultrasonic velocities (V_p and V_s) and seismic attenuation are being conducted in a triaxial deformation apparatus at pressures of 0 MPa to 170 MPa, temperatures of 25°C to 160°C, room-dry, and with a small differential stress of 5 to 10 MPa. To measure attenuation, we use the forced-oscillation technique by applying small-amplitude (0.1 MPa) sinusoidal stress oscillations at frequencies between 0.05-15 Hz. Attenuation is determined from the phase shift between stress, measured with an internal force gage, and strain, measured with 6 internal radial and axial LVDTs. We verify the accuracy of this technique through calibration experiments on PMMA and aluminum.

PRESENCE AND ROLE OF PARTIAL MELT IN CONTINENTAL RIFTING

Gaherty J., D. Shillington, E. Hopper, B. Holtzman, C. Havlin, N. Accardo, G Jin

It is hypothesized that partial melting in the upper mantle plays a critical role in the rifting of continental lithosphere. Evidence of surface volcanism varies widely between rifts, however, making it difficult to fully assess the role of melt in different rift environments. Over the past decade, several seismic imaging experiments have enabled the systematic evaluation of the shear velocity of the crust and upper mantle. Coupled with new algorithms for estimating the thermal and compositional contributions to velocity variations, these images enable assessment of the distribution of partial melt in the upper mantle and its role in extension in diverse rift environments. We evaluate the thermal state and likely melt distribution in four diverse rift environments: incipient and mature portions of the East African Rift (Malawi and Ethiopia, respectively), where stable continental lithosphere is rifting; Papua New Guinea, where accretional lithosphere is being incised by rift propagation; and the Gulf of California, where an ancient arc has rifted and evolved to seafloor spreading. We model shear-velocity images of the lithosphere-asthenosphere system in terms of temperature, grain size, and melt distribution in these different systems using a thermodynamically self-consistent algorithm, and evaluate the role of melt in accommodating extension.

CRUSTAL STRUCTURE OF THE NORTHERN HIKURANGI MARGIN FROM MARINE SEISMIC REFLECTION IMAGING AND ONSHORE-OFFSHORE SEISMIC TOMOGRAPHY: IMPLICATIONS FOR MEGATHRUST HETEROGENEITY AND OVERPRESSURE IN A REGION OF SHALLOW SLOW EARTHQUAKES

Gase A., H. Van Avendonk, N. Bangs, D. Okaya, S. Henrys, D. Barker, K. Jacobs, S. Kodaira, G. Fujie, A. Arnulf

The northern Hikurangi margin is the site of recurring shallow slow slip events and historic tsunami earthquakes. We present results of a trench perpendicular multichannel seismic and onshore-offshore wide-angle seismic transect in northern Hikurangi margin, acquired during the Seismogenesis at Hikurangi Integrated Research Experiment (SHIRE). We invert wide-angle P-wave (VP) traveltime arrivals recorded on 18 ocean-bottom seismometers and 13 IRIS/PASSCAL seismometers to estimate VP structure to depths up to ~25 km. A zone of elevated VP below a major out-of-sequence thrust at Tuaheni Ridge is interpreted as a subducted seamount. Ocean-bottom and onshore receivers down-dip of the subducted seamount show low VP in the prism (~2-3.5 km/s) and a shadow zone. The shadow zone (i.e. velocity inversion) coincides with the landward appearance of a reflective zone near the subduction interface. Wide-angle reflections after the shadow zone are attributed to the subduction interface, subducted basement, and the subducted Moho. The shadow zone may result from elevated pore pressures in the lower prism and/or deep under-consolidated, basally accreted sediments down-dip of a subducting seamount. These features coincide with the source regions of shallow slow-slip events and tectonic tremor, implying that megathrust heterogeneity and elevated pore pressures promote slow earthquake nucleation.

FROM RIFTING TO SUBDUCTION: SUBDUCTION INITIATION AT THE PUYSEGUR TRENCH, NEW ZEALAND

Shuck B., S. Gulick (presenter), H. Van Avendonk, M. Gurnis, J. Stock, R. Sutherland, E. Hightower, J. Patel

The Puysegur margin exhibits several characteristics of a subduction zone, including ongoing plate convergence, an active Benioff zone, and adakitic volcanism. Plate reconstructions show that the margin has experienced a complicated tectonic transformation from rifting to seafloor spreading, to strike-slip motion, and most recently to incipient subduction, all in the last ~45 million years. Here we present new seismic images from the South Island Subduction Initiation Experiment (SISIE) which surveyed the Puysegur region during February-March, 2018. SISIE acquired 1252 km of deep-penetrating multichannel seismic (MCS) data on 8 lines, including 2 critical dip lines which extend from the incoming Australian plate to across the forearc Solander Basin. We include crustal velocity models using University of Texas ocean bottom seismometer wide-angle data. Our preliminary MCS profiles reveal: (1) Solander Basin crust is extended and tilted on large normal faults. We infer that the basement here is thinned continental Campbell Plateau crust formed during Eocene rifting. (2) In the south, we see thinner crust stretched over a wider distance, therefore we can confirm that rifting propagated from south to north. (3) We see active underthrusting and a décollement on both the northern and southern lines with a well developed accretionary prism to the north albeit with many indication of obliquity and a role of strike-slip tectonics within the forearc around the Snares Zone.

3D SEISMIC IMAGES OF DOUBLE BSRs AT THE NORTHERN HIKURANGI MARGIN AND THE IMPLICATIONS FOR SUBDUCTION PROCESSES

Han S., N. Bangs, J. Edwards, H. Tobin, G. Moore, E. Silver

Bottom simulating reflector (BSR), that marks the base of gas hydrate stability zone, is widely observed at continental margins. At some locations, double or multiple BSRs are observed, yet their formation mechanisms are not well understood. In January and February of 2018 we acquired a 3D seismic data volume within a 14.7 x 60 km survey area aboard the R/V Langseth along the Hikurangi margin offshore the east coast of the North Island of New Zealand. From the 3D migrated images, we observe double BSRs beneath the Tuaheni basin and several thrust ridges with various reflection characteristics and a range of separating time from the main BSR. The formation of these double BSRs is likely related to the depositional, slumping, and tectonic uplift processes at the northern Hikurangi subduction margin. Our study demonstrates the close tie between fluid/gas migration and the dynamic subduction processes at Hikurangi margin.

VARIATIONS IN THE APPARENT COEFFICIENT OF FRICTION, HIKURANGI MARGIN, NEW ZEALAND

Harris R., A. Trehu, H. Rabinowitz

Marine heat flow measurements combined with heat flow estimates from bottom simulating reflections and continental bottom hole temperatures are used to constrain thermal models of subduction at the Hikurangi margin along the IODP Expedition 375 drilling transect. Heat flow data landward of the deformation front show a broad westward decline in values consistent with landward thickening of the margin and advection of cold material downward. To better understand the long-wavelength heat flow variations and the thermal regime we constructed a two-dimensional finite element model using the source code developed by Wang et al. (JGR, 1995) that solves the steady-state heat conduction-advection equation. We incorporate shear heating along the plate interface and vary the effective coefficient of friction. In our preferred model the effective coefficient of friction increases from 0.06 to 0.18 at 50 km landward of the deformation front. If the intrinsic coefficient of friction is 0.4, appropriate for clays, an effective coefficient of friction of 0.06 implies that the pore pressure ratio is close to 0.9 consistent with fluid overpressures. This transition occurs near the down dip end of observed slow slip providing further support for the idea that slow slip is enabled by overpressures.

HOT SLAB TIME MACHINE: PETROCHRONOLOGIC EVIDENCE FOR PROTRACTED AMPHIBOLITE-FACIES METAMORPHISM OF THE CATALINA SCHIST (SANTA CATALINA ISLAND, CA)

Harvey K., P.G. Starr, S. Walker, S. Penniston-Dorland, M.J. Kohn, E. Baxter

The role of transient tectonic processes (e.g. nascent subduction, slab rollback, delamination, subduction erosion, etc.) in the formation of many subduction-related terranes is poorly understood, yet critically important for ascertaining the relationship between paleo- and modern subduction. The Catalina Schist is interpreted to be an exhumed subduction interface. It consists of km-scale sub-horizontal thrust sheets ranging from lawsonite-albite to upper amphibolite facies. While the thermal gradients recorded by the lower grade units ($\sim 10\text{-}12^\circ\text{C}/\text{km}$) are broadly consistent with those observed in other exhumed terranes, the anomalously high temperature recorded by the amphibolite facies units is difficult to reconcile with steady-state subduction. Mélange blocks throughout the terrain record different peak metamorphic conditions that may be related to changes in the thermal structure of the slab. The peak metamorphic conditions of four blocks that span the range of high-T thermal gradients recorded by the terrane were estimated using Zr-in-rutile thermometry and quartz-in-garnet barometry, and range from $624\text{-}760^\circ\text{C}$ ($\pm 9\text{-}10^\circ\text{C}$) and $1.18\text{-}1.64$ GPa ($\pm 0.01\text{-}0.02$). Sm-Nd garnet geochronology was used to determine the timing of these conditions. Ages for three amphibolite-facies rocks span from 120.4 ± 1.0 Ma to 108.6 ± 1.7 Ma, and suggest that thermal gradients between $\sim 13\text{-}17^\circ\text{C}/\text{km}$ were sustained at the slab interface for at least 12 Myr. A fourth garnet blueschist block preserves a significantly older age of 151.7 ± 1.4 Ma, but a similarly high thermal gradient of $\sim 13^\circ\text{C}/\text{km}$. These results provide new insight into the thermo-tectonic evolution of the Catalina Schist, including the roles of non-steady state tectonic processes.

REVISITING THE 1964 GREAT ALASKA EARTHQUAKE IN A SLAB-DRIVEN FOREARC SLIVER-ESCAPE TECTONICS FRAMEWORK

Haynie K., M.A. Jadamec

Investigations of the correlation between individual subduction zone parameters and great earthquakes indicate no one parameter is involved, implying a coupled mechanism. We use 3D simulations of the natural subduction system in Alaska to examine the tectonic framework within which the 1964 Great Alaska Earthquake occurred. Models test the relative effect of increased coupling in the flat slab apex zone (10^{21} - 10^{23} Pa·s) and resistance along the Denali fault shear zone (DFSZ), which forms the leading edge of the Wrangell block forearc sliver. A coupled slab apex and weak DFSZ provide the best fit to observations. Results suggest the 1964 Earthquake occurred along a compression zone bounded by the trench and buttress in the Denali fault and follows the trajectory of the slab apex. In this system, the Wrangell block is the effective upper plate involved in the great earthquake, not North America proper. Consistent with analog models, the plate interface motion is intrinsically connected to the intracontinental shear zone via the intervening forearc sliver. Thus, the 1964 Alaska Earthquake occurred above a slab apex in a forearc sliver-escape tectonics system. This implies forearc sliver dynamics are important for hazard assessment of great earthquakes in regions of oblique subduction.

GRAVITATIONAL MODELING OF CRUSTAL STRUCTURE AND COMPOSITION OF THE PUYSEGUR MARGIN, SOUTH ISLAND, NEW ZEALAND: INSIGHTS INTO SUBDUCTION INITIATION

Hightower E., M. Gurnis, H. Van Avendonk, J. Stock, S. Gulick, R. Sutherland, B. Shuck

The Puysegur subduction zone is a young system with a well constrained tectonic history that is making the transition from a forced to a self-sustaining state, where slab pull begins dominating the force balance. The South Island Subduction Initiation Experiment imaged the Puysegur Trench using multichannel seismic (MCS) reflection and ocean-bottom seismometer (OBS) refraction. Horizons for seafloor, basement, and sediments were picked from two MCS profiles crossing the plate margin to constrain the structure of the density models used for gravity modeling. We constrained Moho depth with velocity models derived from the OBS data. We forward modeled the gravity and compared it to satellite gravity to determine compositional and structural heterogeneities. The large negative gravity anomaly over the Snares Zone requires a low-density root beneath Puysegur Ridge, which is composed of continental crust, the eastern half of which was likely rifted off the Campbell Plateau. This block appears less dense than normal Campbell Plateau crust, perhaps due to faulting. The western half of the ridge may be entirely accreted sediment. Both the OBS and gravity data support the presence of serpentinitized mantle beneath the AU plate in the north. The southern line is consistent with Puysegur Ridge and the Solander Basin basement being continental crust, though basaltic volcanic intrusions may account for the higher density in the south. The continental composition of Puysegur Ridge implies large density contrasts are key for subduction initiation; subsidence of the buoyant crust implies the system is transitioning to a slab pull state.

THE EFFECTS OF THICK SEDIMENT UPON CONTINENTAL BREAKUP: KINEMATIC AND THERMAL MODELING OF THE SALTON TROUGH, SOUTHERN CALIFORNIA

Han L., J.A. Hole (presenter), R.P. Lowell, J.M. Stock, G.F. Fuis

A one-dimensional time-dependent numerical model was developed to simulate the rifting process and thermal evolution of the Salton Trough. The rifting model is based upon a new seismic velocity model. It postulates that the addition of underplated mafic magma and deposited sediment compensate for thinning of the crust during extension. The crustal rheology calculated from lithology and the modeled temperature shows that deformation in the lower crust in the Salton Trough is currently ductile. The same extension mechanism could persist for millions of years if a sufficient sediment supply persists. Rapid sedimentation delays the final breakup of the continental crust and prevents the initiation of seafloor spreading by maintaining the thickness of the extended crust. This process probably affected passive continental margins globally.

SLOW SLIP AND TREMOR: A REVIEW OF THE ROLE OF WATER EXPELLED FROM SUBDUCTING PLATE

Hyndman R.

In this presentation I will deal mainly with the deep ~35 km continuous band of slow slip and tremor that occurs in hot subduction zones, but also comment on other subduction zones and on shallow near-trench occurrences of VLFE. My first point is that there is a gap between the band of ETS and the seismogenic zone in SW Japan and Cascadia, and perhaps other hot subduction zones where the seismogenic zone is thermally limited to a relatively shallow depth down dip. ETS occurs where the temperatures are sufficiently high for ductile behaviour (occur at 500-550C compared to the thermal seismogenic limit of about 450C). There is not a continuous transition between seismic and aseismic ETS slow slip behaviour. At cold subduction zones, the seismogenic zone may reach the forearc mantle corner and, where ETS occurs, there may be not be a gap. The question then is, what controls the location of ETS for SW Japan, Cascadia, and other hot subduction zones? We have concluded that the answer is that ETS is restricted to the region of the forearc mantle corner. There is excellent correspondence in the locations of ETS and the corner. Thermal models combined with laboratory data on dehydration P-T conditions indicate large fluid expulsion from dehydration of hydrated mineral assemblages in the downgoing plate at about that depth for hot subduction zones (deeper for cold subduction zones). However, this fluid must be focussed at the corner to explain the precise correspondence. We have proposed that deeper than the corner, ocean plate dehydration fluid is blocked from rising vertically by low permeability serpentinite in the overlying forearc mantle. The fluid is channelled up dip in the high permeability oceanic crust, and is released at the corner where it is no longer blocked by low permeability serpentinite (Figure 1). Slip and tremor may occur in spite of the high temperatures, because of “fault valve” buildup and simultaneous release of high pore pressure and shear stress.

Concentrated fluid expulsion above the forearc mantle corner is indicated by: (a) Evidence for quartz deposition in the crust above the corner in V_p/V_s (Poisson's Ratio) tomography data (note NZ example of quartz outcrop, and possible importance for gold formation that requires very large amounts of fluid); (b) A high electrical conductivity plume above the corner from magnetotelluric data.

The updip near trench region of slow slip and very low frequency earthquakes (VLFE) in SW Japan also may be in an area of normally aseismic behaviour. However, in this case it is because of stable sliding clays that occur at temperatures below 100-150C. These temperatures occur on the thrust well landward of the trench in SW Japan, and the VLFEs occur where stable sliding clays should be present. Again, buildup and release of pore pressure may give slow slip and VLFEs. VLFEs have not yet been observed at Cascadia where the deformation front area is very hot, over 250C. They may not occur because any stable sliding clays have already been dehydrated near the trench, and seismogenic behaviour may extend to near the trench (but need better data and analysis).

SLOW EARTHQUAKES WORLDWIDE: DATABASE AND INTERPRETATION WITH THE SCIENCE OF SLOW EARTHQUAKES PROJECT

Satoshi I.

Since 2016, we are conducting JSPS Project for Science of Slow Earthquake in Japan (<http://www.eri.u-tokyo.ac.jp/project/sloweq/en/>). This project intends to improve our understanding on slow earthquakes, which have been detected in many places worldwide. We integrate conventional fields of geophysics, seismology, geodesy, and geology with non-equilibrium statistical physics, and try to explain the mechanisms, environmental conditions and principles of slow earthquakes. In addition to individual projects of observations, experiments, and theoretical works, we convene annual international joint workshops and many small to moderate gathering of researchers. The workshop in 2019 will be held in Sendai, in September 21-23.

The major product from this project is the slow earthquake database (Kano et al., SRL, 2018; Tanaka et al., AGU, 2018). In database website (<http://www-solid.eps.s.u-tokyo.ac.jp/~sloweq/>), users can visualize source locations of slow earthquakes on Google Maps, access to the information of the original papers, and download them with our unified format. As of January 2019, 46 catalogs are registered in our database and categorized by the region (Japan, Cascadia, San Andreas, Mexico, Chile, New Zealand, and Taiwan) and phenomenon (tremors, low-frequency earthquakes, very low-frequency earthquakes, slow slip events, and related phenomena like repeating earthquakes). We are accepting contributions from world researchers making their catalogs for similar phenomena.

In my own study in this project, I am developing a unified interpretation of broadband slow earthquakes, which integrate differently named slow phenomena observed in different frequency ranges, as a spatially extending slow slip with high-frequency fluctuations like a Brownian motion. I will explain the background, scaling relations, and some predictions derived from this model.

WIDTH OF IMBRICATED THRUST BLOCKS AND THE STRENGTH OF ACCRETING SEDIMENTS AT SUBMARINE WEDGES

Garrett I., G. Moore

We study the mechanical processes and material properties that control the spacing of major imbricate thrust faults at accretionary wedges using 2-D, finite-difference models. Model results show that the width of individual thrust blocks are maximum when the thrusts first form at the toe of the wedge, and then decrease landward in proportion to the mean shortening rate of the portion of the wedge including and forward of the thrust block. The maximal, initial thrust block width w_0 increases linearly with the thickness of the incoming sediment layer, increases with the coefficient of friction of the sediments, and shows a weak inverse relation with $(1-\lambda)\mu_b$, where λ is pore-fluid pressure ratio and μ_b is the coefficient friction along the basal décollement. Elastic stress solutions determine the form of functions of the above properties that are used to derive scaling laws that explain the model predictions. Estimates of initial thrust block widths from seismic reflection profiles of the Aleutian, Cascadian, Nankai, New Zealand, and Makran accretionary prisms show an increase with incoming sediment thickness, in support the results of this study as well as prior studies. We are developing a method to use observed widths and wedge tapers with our new scaling laws as well as critical Coulomb wedge theory to estimate the relative frictional strengths of the sediments and the basal décollements near the toe of these accreting systems.

EFFECT OF CONTRASTING STRENGTH FROM INHERITED CRUSTAL FABRIC ON THE DEVELOPMENT OF RIFTING MARGINS: THE EXAMPLE OF THE NORTHEASTERN CANADIAN MARGIN

Jammes S., L. Lavier

The Northeastern Canadian continental crust is the result of a series of accretionary orogens during the Proterozoic, juxtaposing terranes of different composition and crustal fabrics. During the Mesozoic, the northward propagation of the Atlantic Ocean led to the formation of the Northeastern Canadian margins characterized by a highly variable architecture. If several studies suggest that inheritances control the localization and development of rift structures, the processes remain unclear. To address this question we conducted a multidisciplinary study combining the analysis of geological and geophysical data of the Northeastern Canadian margin with numerical modeling experiments of lithospheric extension including strength variation from inherited crustal fabric within their initial conditions. The orientations of the crustal fabrics are compatible with kilometeric-scale heterogeneities observed in seismic reflection data.

Our study demonstrates that inherited crustal fabrics can explain: 1) the different deformation processes observed during the stretching phase (formation of horst-and-grabens versus core-complexes), 2) the diversity of thinning processes involving detachment faulting, sequential normal faulting or alternative models, 3) the resulting geometry of the margin. Finally, our results are compared to the Northeastern Canadian margin and insights on the variability of architecture of the margin are discussed.

RECEIVER FUNCTION IMAGING OF MAGMATIC- AND SUBDUCTION-RELATED STRUCTURES BENEATH ARC VOLCANOES: A CASE STUDY AT CLEVELAND VOLCANO, ALASKA

Janiszewski H., L. Wagner, D. Roman

Cleveland Volcano is one of the most active volcanoes in the central-Aleutian island arc and represents one of the shallow-end members of depth to subducting slab at only ~ 65 km below the volcano. It was the site of a temporary deployment of twelve broadband seismometers from August 2015 - July 2016. We calculate P-to-s receiver functions using these as well as two permanent Alaska Volcano Observatory stations, which have operated since 2014, to determine new seismic constraints on the crustal structure beneath Cleveland Volcano and the depth to the subducting crust. At Cleveland Volcano we image a clear P-to-s conversion from the Moho discontinuity. However, its arrival time relative to the initial P-wave typically varies up to two seconds at a given station with later arrivals systematically corresponding to ray paths that have passed through crust directly beneath the volcano. The most likely explanation is that slow shear-wave velocities associated with the magmatic system beneath Cleveland Volcano contribute to the travel time variability, with perhaps a secondary contribution from smaller variations in Moho topography.

LITHOLOGY AND CEMENT CONTROLS ON THE EVOLUTION OF COMPRESSIONAL WAVE VELOCITY AND POROSITY IN INPUT MATERIALS AT NORTHERN SUMATRA AND OTHER SUBDUCTION ZONES

Jeppson T., H. Kitajima

The mechanical, physical, and frictional properties of incoming materials play an important role in subduction zone structure and slip behavior because these properties influence the strength of the accretionary wedge and megathrust plate boundary faults. Incoming sediment sections often show an increase in compressional wave speed (V_p) and a decrease in porosity with depth due to consolidation. However, variations in these properties are also controlled by lithology, composition, cementation, and diagenesis. In North Sumatra hemipelagic sediments sampled during Expedition 362 (Units I-II), porosity generally decreases (80% down to 30%) and V_p increases with depth. In pelagic Unit III, sediments begin to deviate from this trend and both higher and lower porosities (6-60%) are observed in this unit and velocity increases by 600 m/s. In Unit III and IV, velocity increases and porosity decreases with increasing CaCO_3 content, suggesting that the evolution of V_p and porosity may be related to the extent of calcite cementation. We compare data from the Sumatra margin with data collected at the Nankai Trough and Aleutian Trench to elucidate the effects of cementation, composition, and lithology on the physical properties of the incoming section and their impacts on the slip behavior of megathrust plate boundary faults.

IMPLICATIONS OF SUBDUCTION OBLIQUITY TO THE INFERENCES OF SEISMIC ANISOTROPY IN THE MANTLE WEDGE

Kenyon L., I. Wada

This study aims to systematically quantify the effect of subduction obliquity on the patterns of mantle flow, olivine crystal preferred orientation (CPO), and seismic anisotropy in the creeping part of the overriding mantle wedge in subduction zones. Previous studies of mantle wedge flow patterns using numerical models have shown that when the subduction direction is oblique to the margin, coupling between the subducting slab and the overriding mantle induces complex 3-D mantle wedge flow pattern [e.g., Kneller and van Keken, 2008; Wada et al., 2015]. In this study, we develop a series of 3-D kinematic-dynamic models for generic subduction systems by varying subduction obliquity and other subduction parameters, such as slab dip and slab age. We pay special attention to adopting a model domain that minimizes the effects of boundary conditions on the mantle wedge flow pattern. For a given mantle flow pattern, we compute the pattern of olivine CPO in the mantle wedge, using the crystallographic code [Kaminski et al., 2004]. The resulting CPO is complex and varies between the outflow and inflow areas and with distance from the slab in the mantle wedge. We plan to calculate S-wave splitting parameters using the calculated CPO patterns and quantify the variations in the splitting parameters with subduction obliquity.

PRELIMINARY PETROLOGIC AND MICROSTRUCTURAL CHARACTERIZATION OF A METAMORPHIC SECTION BENEATH THE SAMAIL (OMAN) OPHIOLITE: RESULTS FROM THE OMAN DRILLING PROJECT HOLE BT1B

Kotowski A., E. Bos Orent, M. Cloos

The Oman Drilling Project obtained cores from the Samail Ophiolite to address questions about ocean crust formation, alteration, and emplacement on land. Phase I drilling at Hole BT1B recovered 200 m of listvenite and serpentinite, several meters of cataclasites of the Basal Thrust, and 100 m of sub-ophiolite metamorphics (30 m of sediments, 70 m of mafic volcanics). Phyllitic metasediments (n=6) are thinly laminated. Cm-scale isoclinal folds with fishhook and eye structures indicate transposed layering and large shear strains. Petrographic, EMPA, and XRD analyses (microdrilling, n=139) indicate mineralogies are varied proportions of quartz, albite, phengitic (3.1-3.4 Si a.p.f.u) white mica (muscovite), chlorite, titanite, ilmenite ± epidote. The mafic section (n=29) lacks pseudomorphs of magmatic mineralogies suggesting it is a highly distorted, possibly glassy volcanic protolith. The mineral assemblage is amphibole, epidote, albite, and chlorite. Amphiboles are compositionally zoned, with magnesio-hornblende cores and actinolite rims, and actinolite cores with chlorite rims. Ductile fabrics are cross-cut by veinlets revealing evidence for CO₂- and H₂O-rich fluids in fractures, associated with zones of microbrecciation. The metamorphics record a dynamic period of recrystallization during early stages of subduction along a hot geotherm to ~450-550°C and 4-7 kbar. The retrograde history evolves from ductile to localized brittle deformation under greenschist facies conditions, probably related to unroofing.

EXPERIMENTAL CONSTRAINTS ON MECHANICAL BEHAVIORS OF THE INNER ACCRETIONARY PRISM SEDIMENTS AT THE NANKAI SUBDUCTION ZONE

Kuo S., H. Kitajima, M. Kitamura

The Integrated Ocean Drilling Program (IODP) Nankai Trough Seismogenic Zone Experiment (NanTroSEIZE) aims to investigate the mechanics of earthquakes and faulting by drilling through an active plate boundary megathrust. A deep riser hole at Site C0002 located ~35 km landward from the trench has reached 3058 meters below seafloor (mbsf) by drilling through the Kumano forearc basin and the underlying inner accretionary prism. In this study, we aim to develop an experimental-based method to constrain the possible in situ strength, stress, and deformation modes of the sediments at Site C0002. We performed an isotropic consolidation experiment and a suite of triaxial compression experiments on samples with porosity of ~20% at either 20°C or 60°C. In the isotropic loading test, the sample yields at effective pressure of 100 MPa (P^*). In triaxial loading tests, the samples deformed at effective pressure (P_e) less than 28 MPa exhibit mechanically brittle behavior. The sample at P_e of 58 MPa shows ductile behavior with strain hardening. With an application of the modified Cam-clay model, our results reveal that the accretionary prism rocks at ~2 km depth reside in a stress regime that favors brittle deformation at both hydrostatic P_p and overpressure condition. Based our newly-developed empirical relation between P^* and porosity, we predict that the deformation mode of the Kumano basin is generally ductile, whereas the accretionary prism rocks deform more brittle as the depth increases.

THE IRES MALAWI RIFT PROJECT: SYNTHESIS AND FUTURE DIRECTIONS

Laó-Dávila D., E.A. Atekwana, M.G. Abdelsalam, P.R.N. Chindandali, F. Kolawole, S.G. Johnson, S.M. Dawson

The IRES Malawi Rift Project was established to investigate the role of pre-existing structures in the localization of strain during the early stages of continental rifting. Inherited structures have been recognized to affect the propagation, segmentation, and location of continental rifts. However, it is still unclear how the orientation of these structures influence strain accommodation. To study this problem, we analyzed SRTM-DEMs, aeromagnetic, electrical tomography, and structural data from the Malawi Rift. At the regional scale, we found that the rift can be hierarchically divided into first-order and second-order segments controlled by the inherited lithospheric heterogeneity. Results from the Karonga region suggest that the orientation of the Precambrian Mughese Shear Zone influences strain accommodation and has implications for seismic hazard. The 2009 Karonga earthquake follows a 35 km-long regional magnetic lineament in the basement and aligns with a zone of deformation apparent in the electrical resistivity inversion models. In central Malawi, the aeromagnetic-defined foliation and the SRTM-defined regional jointing patterns control the orientation of the Bilila-Mtakataka and Chirobwe-Ntcheu faults, the location of linkage zones, and the displacement of the fault segments. Future work should focus on constraining the ages of fault growth and strain rates within the Malawi Rift.

THE SECOND HALF OF PLATE TECTONICS: 3-D MAPPING OF THE REMNANT "PALEO-PACIFIC" SLABS IN THE LOWER MANTLE UNDER EAST ASIA AND ITS TECTONIC IMPLICATIONS

Liu Y., J. Suppe

It is often suggested that the Paleo-Pacific plate subduction dominated the Jurassic-Cretaceous tectonics of East Asia, creating a 6000-km-long arc system. Nevertheless, the nature of the Paleo-Pacific are controversial, because it had entirely subducted by Eocene. We use seismic tomography models to map the subducted slabs in 3-D and tie them with geologic records.

We identify three major slabs in the lower mantle: Izanagi, Hunan, and Taipei. The Izanagi slab is a N35E-trending slab wall located at 1000-2200 km depths beneath Far East Russia and Northeast China. To the south, the Hunan slab is separated by a gap from the Izanagi. It strikes N15E and dips vertically. Its depth ranges from 1450 km to the base of the mantle. Projected onto surface, this slab spans the North China, South China, and northern Vietnam. The Taipei slab dips moderately to the south, and strikes ENE at shallow depths (1050-1500 km) and ESE at 1600-2000 km depths. It lies under the Taiwan Island and the Philippine Sea with a minimal width of 2200 km. The so-called Paleo-Pacific consists of at least three slabs with different history. Their geometry and spatial relationship provide independent evidence for East Asian tectonics, including: 1) extensive, Jurassic-Early Cretaceous arc magmatism along the entire margin, 2) subduction cessation in South China in early Late Cretaceous, 3) ridge subduction, 4) rotational, retreating trench during the Taipei slab subduction, 5) opening of the East Asia Sea, and 6) exotic terrane accretion.

STRUCTURE, DYNAMICS, AND EVOLUTION OF THE EASTERN NORTH AMERICAN MARGIN: RESULTS FROM THE MAGIC PROJECT, CENTRAL APPALACHIANS

Long M., M.H. Benoit, R.L. Evans, S.D. King, E.Kirby, J.Aragon

The surface geology of eastern North America is extraordinary in its complexity. This complexity reflects a wide range of tectonic processes that have operated in the region over the past billion years, including episodes of subduction and rifting associated with two complete Wilson cycles of supercontinent assembly and breakup. It is poorly known, however, how the deep crust and mantle lithosphere have responded to these tectonic forces over time; furthermore, the persistence of Appalachian topography through time remains a major outstanding problem in the study of landscape evolution. I will present recent results from the MAGIC project, a multidisciplinary collaboration that includes a broadband seismic and magnetotelluric deployment across the central Appalachians in Virginia, West Virginia, and Ohio, along with geodynamic modeling and geomorphology investigations. These results inform a suite of fundamental science questions articulated by the GeoPRISMS program in the context of the Eastern North American Margin (ENAM) focus site.

DIFFUSION CHRONOMETRY IN SANIDINE: HELPING UNRAVEL THERMAL HISTORIES OF LARGE SILICIC MAGMA RESERVOIRS

Lubbers J., A. Kent

Correctly interpreting processes that govern how silicic magma is generated, stored, and differentiated within the upper crust is fundamental to understanding explosive eruptions. Constraining the timescales on which these processes occur can provide insight with regards to eruption timing and interpretation of volcano monitoring data and also constrain the long-term conditions of magma storage. Despite the importance of understanding these conditions, the thermal evolution of large silicic magma reservoirs and the timescales on which they exist in an eruptible state are not fully understood.

From this ambiguity, two end-member hypotheses have been proposed: (1) Magma reservoirs spend the vast majority of their time in a state of 'cold storage' at near solidus temperatures, where they are not eruptible, and experience punctuated thermal events that generate eruptible magma. (2) Magma reservoirs spend the vast majority of their time in a state of 'warm storage' at temperatures much closer to the liquidus, where they contain a significant and eruptible melt fraction throughout much of their history.

Here we utilize electron probe micro-analyzer derived X-Ray maps of sanidine crystals and diffusion chronometry to better constrain the thermal evolution of the 900 km³ Kneeling Nun Tuff (New Mexico, USA) and discern how some of the largest volcanic eruptions on the planet are formed. Recent work has suggested that the Kneeling Nun Tuff, prior to eruption, underwent roughly 600,000 years of magma assembly between the granitic solidus (680-700°C) and the temperature of titanite crystallization (720-730°C). Diffusion timescale estimates generated from sanidine grains, after comparison with previous work, indicate that the Kneeling Nun Tuff spent the vast majority of its time in a state of cold storage, unable to erupt until thermal rejuvenation of the reservoir immediately prior to eruption.

TILT AND COMPLIANCE CORRECTIONS FOR THE ENAM BROADBAND OBS INSTRUMENTS

Lynner C., T. Guajardo, H. Janiszewski, Z. Eilon

As part of the Eastern North American Margin Community Seismic Experiment (ENAM-CSE), 30 broadband ocean-bottom seismic (OBS) instruments were deployed in the waters off-shore of North Carolina. All of the OBS instruments were located between ~1.3 km and ~5.2 km water depth. When dealing with OBS data, it is often necessary to perform pre-processing corrections in order to take full advantage of the dataset. The most important corrections are generally for tilt and compliance. Errors associated with tilted instruments result in the transference of energy from the vertical component to the horizontal components and vice versa. The compliance signal acts to obscure seismic signals recorded on the vertical component. Both must be corrected in order to reliably use the OBS data for analyses such as surface wave tomography. All of the ENAM-CSE instruments were equipped with differential pressure gauges that we use to remove the compliance signal from the vertical component. We also calculate the orientation and magnitude of tilting from the horizontal components of each station. After correction, the seismic waveforms are far cleaner and clear seismic phases emerge. Here we present corrections for the ENAM-CSE OBS instruments.

THE EFFECTS OF BACK-ARC SPREADING ON ARC MAGMATISM

Magni V.

Mantle flow is a key feature that can affect melt production and composition in and around subduction zones. In this study, I use three-dimensional numerical models to investigate the role of mantle flow on subduction-related volcanism during back-arc extension. Results show that for a period of about 10-15 Myr during back-arc basin formation and spreading a wide convection cell brings mantle that has already partially depleted at the back-arc to the mantle wedge. Before and after this phase, the mantle reaching the sub-arc melting region is fertile. Thus, changes in back-arc activity and mantle flow pattern can be responsible for changes in magmatic composition and the amount of magmatism at the arc. These results are consistent with many examples of present-day subduction zones, in which phases of actively spreading back-arc correspond to a gap or a decrease of the arc volcanic activity.

NORTHERN LAU BASIN TECTONICS AND VOLCANISM ALONG A PROPAGATING SLAB TEAR

Martinez F., J. Conder, J. Caplan-Auerbach

The northern end of the Tonga Trench is the type-example of subduction termination by a propagating slab tear, a globally important class of plate tectonic boundary termed a subduction-transform edge propagator (STEP) fault [Govers and Wortel, 2005]. STEP fault tectonics predict that shear deformation generated along the ends of subduction zones can be broadly distributed within the adjacent backarc basin within rifts, spreading centers and possibly rapidly rotating microplates. Viscous coupling of these rapidly evolving microplates with the underlying mantle implies complex mantle flow patterns. Occurrences of unusual geochemical and hydrothermal signatures (associated with hotspot, subduction, and regional isotopic domains) in the northern Lau Basin have long been used to examine the broad pattern of mantle flow around a torn slab edge, however, possible effects of local backarc tectonics on this flow have never been examined because the local tectonics have yet to be resolved. The STEP fault model schematically predicts deformational kinematics associated with shear-driven tractions acting on microplates in the northern basin and the strain pattern near the trench-STEP fault corner of the backarc basin. Here we explore the possible nature of deformation and tectonic controls on mantle flow leading to the distinctive volcano-tectonic character of the northern Lau Basin. As the type-example of this common form of subduction termination, the northern Lau Basin serves as an active analog for other less studied and relict cases.

RIFTING EVOLUTION OF THE EASTERN BLACK SEA BASIN FROM LONG-OFFSET SEISMIC REFLECTION DATA

Monteleone V., T.A. Minshull, H. Marín Moreno

In the Eastern Black Sea (EBS), timing and kinematic of rifting are still debated due to the general lack of constrain over the deep stratigraphy of the basin and its underlain basement. In this study, we use long-offset seismic reflection data to: i) define crustal types underlying the central basin and their lateral extension, and ii) understand rifting spatial and temporal distribution. Initial results, combining basement morphological analysis with the definition of syn-rift structural and stratigraphic elements, show a change from stretched continental crust (NW) to an interpreted continent-ocean transition and then to oceanic crust (SE). Magnetic anomaly data support the presence of magnetised crust in the central and SE part of the EBS, where post-rift sequences directly overlies the basement. Within the stretched continental domain, the deep stratigraphic infill shows the presence of two syn-rift sequences recording an initial extension focusing within isolated depocentres and, subsequently, strain focusing along the main basin-bounding faults and migrating towards the basin axis. The early post-rift sequences (Palaeocene-Eocene), and the lower Maykop Formation sequence (Oligocene), show that extension continued up to Oligocene in the NW and along the major basin-bounding faults, whereas breakup may have occurred before their deposition in the SE.

COMPLETING THE MEGATHRUST CYCLE

Newman A., T. Hobbs, C. Kyriakopoulos, L. Feng, M. Protti, T. Dixon

Using a 20-year geodetic time history of interseismic activity in Nicoya, Costa Rica, we can now show a rich history of activity along the megathrust we can illuminate the variability of earthquake behavior through the most dynamic component of an earthquake cycle. Here, we will report on the record of locking and slow-slip before the 2012 Nicoya 2012 Mw 7.6 earthquake, the event itself, the afterslip, and then the very strange postseismic sliver transient during the recoupling period. Finally the relocking itself. We will explain the totality of the locking in relationship to other behaviors over time, and discuss the relative similarities between relocking and old locking. By completing the cycle, we are getting at understanding the complete geodetic moment budget allowable from tectonic convergence rather than the 10-20% allowable from seismic only estimates.

SEISMICITY AND SEISMIC VELOCITY STRUCTURE AROUND THE TRENCH AXIS AND OUTER RISE REGION ALONG THE JAPAN TRENCH

Obana K., Y. Nakamura, G. Fujie, S. Miura, S. Kodaira

We have examined seismicity and seismic velocity structure in the incoming/subducting oceanic plate based on ocean bottom seismograph (OBS) observations, which have been conducted in Japan Trench area after the 2011 Tohoku-oki earthquake. The results show that the seismic velocities within the uppermost mantle of the incoming Pacific plate decrease toward the trench axis with spatial heterogeneity, which seems to be related with seismicity within the oceanic mantle. Also, our OBS data provided information about earthquake activity in the shallowest part of the mega-thrust interface and trench-outer rise region along the Japan trench.

INSIGHTS INTO FAULT-MAGMA INTERACTIONS IN AN EARLY-STAGE CONTINENTAL RIFT FROM SOURCE MECHANISMS AND CORRELATED VOLCANO-TECTONIC EARTHQUAKES

Oliva S.J., C.J. Ebinger, C. Wauthier, J.D. Muirhead, S.W. Roecker, E. Rivalta, S. Heimann

Strain in magmatic rifts is accommodated by both faulting and dike intrusion, but little is known of the frequency of dike intrusions in early-stage rifts. We use a new earthquake dataset from a dense temporary seismic array (2013-14) in the ~7 My-old Magadi-Natron-Manyara section of the East African Rift, which includes the carbonatitic Oldoinyo Lengai volcano that erupted explosively in 2007-08. Full moment-tensor analyses were performed on $M > 3.4$ earthquakes (0.03-0.10 Hz band) that occurred during the inter-eruptive cycle. We find two opening crack-type and various non-double-couple earthquake source mechanisms and interpret these as fluid-involved fault rupture. From waveform analysis on the nearest permanent seismic station, we conclude similar rupture processes probably occur over eruptive and inter-eruptive cycles. The repeated and dynamically-similar fluid-involved seismicity, along with intrabasinal localization of active deformation, suggest significant and persistent strain is accommodated by magmatic processes, modulated by tectonic cycles.

HETEROGENEOUS UPPER PLATE EXTENSION IN SOUTH CENTRAL CHILE AND IMPLICATIONS FOR MEGATHRUST FAULT DEVELOPMENT

Olsen K., N. Bangs, A. Trehu, E. Contreras-Reyes

In early 2017, we collected ~5,000 km of multichannel seismic data in south central Chile using a 15.1 km long streamer and 6,600 in³ airgun source. Prestack depth migrated images of these data show extensive normal faulting within the slope and shelf sediment that we have used to infer variations in the shallow stress along the margin. In the 2010 Mw8.8 Maule rupture area (34-39°S), normal faulting begins within the upper 1/3 of the slope (>25 km from the trench), and typically extends landward across the shelf to the end of the seismic line, 80-100 km from the trench. Listric faults with ~0.5-1 km spacing and offsets up to 500 m tend to form in the upper slope, while low offset (~10 m), high angle (55-65°) normal faults form across the shelf. In the 1960 Mw9.5 Valdivia rupture area (39-44°S), normal faulting begins ~15 km landward of the trench, much closer to the toe than in the Maule area. In both regions, normal faults extend through the entire slope/shelf sediment section, but offsets in the underlying middle prism basement are below seismic resolution.

Convergent margins typically undergo compressional stress, but can develop extensional structures due to uplift and oversteepening related to subduction of large topographic features, shortening from faults and folds, and underplating. Other processes such as subduction erosion or gravitational collapse caused by lowering of basal shear stress also result in extension. Due to the subduction of a thick (1-2 km) sediment packet, and the lack of large (>1 km) seamounts or ridges on the incoming Nazca plate in this area, it is unlikely that ridge subduction, tectonic erosion, or major changes in megathrust stress conditions are currently factors in upper plate extension. On the basis of normal fault patterns, sediment may be underplated closer to the toe within the Valdivia region than in the Maule region, leading to important differences in conditions along the plate boundary fault between these two great earthquake regions.

HOW SHALLOWING SLAB DIP COULD PRODUCE EXTENSIONAL UPPER PLATE EARTHQUAKES AFTER A MEGATHRUST EARTHQUAKE?

Oryan B., W.R. Buck

The Tohoku-oki earthquake was one of the strongest earthquakes ever recorded. Up to 60 meters of lateral motion of the sloping seafloor resulted in a tsunami that exceeded predictions and caused one of the costliest natural disasters in history. It was also the first time that extensional aftershocks were observed in the upper plate over a region as wide as 230km.

Such extensional aftershocks are difficult to explain in terms of standard subduction models. We hypothesize that a reduction in the dip angle of the subducting plate can cause upper plate extensional earthquakes. This change in dip angle adds extensional bending stress to the upper plate.

Numerical models testing our hypothesis show that the generation of extensional earthquakes in the upper plate following a megathrust can be the result of a reduction of the dip angle. They also correlate between uplift seen in the upper plate in Japan, migration of the volcanic arc observed in Honshu and the generation of extensional aftershocks in the upper plate.

SURFACE-WAVE ANISOTROPY OF THE EASTERN NORTH AMERICAN MARGIN (ENAM)

Russell J., J.B. Gaherty

The eastern North American margin (ENAM) formed during the breakup of Pangea 175-200 Ma, recording the onset of rifting. The ENAM Community Seismic Experiment (2014-2015) consisted of an onshore/offshore broadband and short-period ocean bottom seismometer (OBS) deployment aimed at better characterizing this relatively understudied region. In this study, we utilize the 28 ENAM broadband OBS to measure Rayleigh-wave phase velocities from ambient-noise (15-40 s period) and teleseisms (40-150 s). Tilt noise is especially high due to the Gulf Stream current; thus, tilt is removed from the vertical component of both teleseismic and ambient-noise waveforms. We observe Rayleigh-wave azimuthal anisotropy of ~2-3% from 15-40 s period with margin-parallel fast directions, orthogonal to predictions of olivine alignment generated by corner-flow at the paleo-ridge. Previous shear-wave splitting observations showed similar margin-parallel splitting, which was attributed to present-day margin-parallel asthenospheric flow. Our measurements are mostly sensitive to the lithosphere, suggesting that this signal is not purely due to present-day asthenospheric flow, but instead, is embedded in the fossilized fabric of the oceanic lithosphere. This observation has implications for the mantle flow field during and immediately after the rifting of Pangea and subsequent opening of the Atlantic Ocean.

BODY AND SURFACE WAVE TOMOGRAPHY OF EASTERN NORTH AMERICAN

Savage B., Y. Shen, B. Covellone

Using full-waveform tomographic modeling methodologies, iterative and non-iterative, 3D wave speed models of the stable North American lithospheric upper mantle and the continental margin are constructed and reveal surprisingly rich and active features. Comparing wave speed models from different data types also suggests slightly different views and interpretations on the formation and subsequent modification / deformation history.

Stable North America consists primarily of fast wave speeds, compressional and shear, but with surprisingly strong variations internally within the craton, up to 5% V_s and 4% V_p , at length scales of around 1 degree. Variations are constrained within the cratonic lithosphere, < 200 km, and are strongest at shallower depths, 75-100 km. Variation in temperature, composition, volatiles, and melt are either not strong enough or violate reasonable assumptions about the cratonic lithosphere.

The addition of a small amount of water-bearing phase, within a Mid-Lithosphere Discontinuity, is able to substantially reduce the wave speeds, thus reproducing the variations within the model. The source of the water bearing phase may be coming from a subducting plate in the transition zone just beneath the eastern portion of North America or from previous mountain building events.

Along the margin between the continental and oceanic lithospheres, the upper mantle shows strong evidence for small scale convection or upwelling punctuated with spatially large cells where raised temperatures and melting are likely present.

IODP DRILLING TO TEST END-MEMBER IDEAS ABOUT THE ORIGIN OF THE ALEUTIAN SUBDUCTION ZONE AND BACKARC BERING SEA REGION

Scholl D., R. Stern, G. Barth, D. Scheirer, K. Martin, M. Malkowski, J. Barron

INTRODUCTION: The Backarc Aleutian Basin (3000-4000 m) lies north of the E-W trending, southward festooning Aleutian Island Arc. Basin and arc are part of the North America plate (NAM). Oceanic crust underlies the basin's thick (3-10 km) sedimentary fill. Two contrasting hypotheses have been proposed for the origin of the basin's oceanic basement:

- (1) basement is a large sector (~500, 000 km³) of accreted (to NAM) oceanic plate of Mesozoic age (Kula/Resurrection?),
- (2) basement formed effectively in-place during an episode of backarc spreading, behind (north of) the forming Aleutian Arc.

Both models call for basin formation in the early Eocene at ~50-55 Ma and coincident with the formation of the Aleutian subduction zone (SZ) and initial growth of its overlying Aleutian Arc.

PRIMARY REGIONAL OBSERVATIONS:

- Physiographically, the Aleutian Arc is a young (Eocene) westward extension of the SW-NE trending Alaska Peninsula constructed of Permo-Triassic and younger crust.
- With respect to the peninsula, paleomagnetic data attest that the Aleutian Arc formed effectively in place,
- The Aleutian Trench-SZ pair is a western, on-strike continuation of the older (Permo-Triassic) Alaska Trench-SZ pair.
- Magnetically, the Aleutian Basin exhibits a prominent pattern of ~N-S-striking spreading anomalies that trend ~normal to that of the Aleutian Arc.
- The Aleutian Basin is structurally framed by continental crust to the north (Beringian Margin) and island-arc structures to the west (Shirshov Ridge) and south (Bowers and Aleutian Ridges).

HYPOTHESIS TESTING: Drilling to basement is technically feasible only at the summits of sediment-buried seamounts. These edifices are not intrusive bodies but constituent parts

PLATE TECTONICS AND MANTLE STRUCTURE OF THE ARCTIC, NORTH ATLANTIC AND PANTHALASSA: RECENT UPDATES

Shephard G., C. Gaina, T. Torsvik, J.I. Faleide

Located at the intersection of major tectonic plates, the kinematic and geodynamic evolution of the Arctic is inherently tied to the North Atlantic and Pacific regions. Collectively, these domains have experienced both widespread and localized deformation since the Paleozoic, including those related to rifting, seafloor spreading, subduction, collision and orogenesis. The region is also characterized by widespread magmatism including the emplacement of large igneous provinces. As such, integrating increasingly detailed regional observations into a digital, global plate motion model demands a multifaceted approach. Here, I will present recent Jurassic to Cenozoic plate reconstruction updates for the Arctic, Pacific and North Atlantic, created via the GPlates software. I will also present a recent workflow that links discrete oceanic subduction events to tomographic images of the deeper mantle, demonstrating how plate tectonics can be iteratively refined in such frontier regions.

SEISMIC IMAGING OF VARIATIONS IN EXTENSION WITH DEPTH AND ALONG-STRIKE IN THE MAGMA-POOR MALAWI RIFT

Shillington D., E. Hopper, N. Accardo, J. Gaherty, C. Scholz, A. Nyblade, C. Ebinger, C. Carchedi, A. Grijalva, D. Borrego, P. Chindandali, R. Ferdinand

Many questions remain regarding controls on variations in extension with depth and along-strike, particularly in early stage rift systems. The Malawi Rift in the southern East Africa Rift System exemplifies an active, magma-poor, weakly extended continental rift. Between 2014-2016, we collected a multi-faceted active- and passive-source seismic dataset across the northern Malawi Rift as part of the SEGMeNT (Studies of Extension and maGmatism in Malawi aNd Tanzania) interdisciplinary experiment. Broadband scattered-wave imaging and wide-angle seismic reflection/refraction data reveal substantial variations in extension with depth, with much more thinning of the lithospheric mantle than the crust. The modest observed reduction in velocity below the rift from both broadband surface- and body-wave imaging can be explained with small thermal perturbations and without melt. Active-source refraction and multi-channel seismic (MCS) reflection data quantify extension accommodated both on the border faults as well as intrabasin faults. Intrabasin faults are large and active and have contributed to extension. Along-strike variations are observed in faulting and in crustal and lithospheric stretching. We will integrate results from passive and active seismic imaging to assemble a complete portrait of lithospheric stretching and evaluate controls on extensional processes here.

THE ROLE OF MANTLE MELTS IN THE PROTRACTED BREAKUP OF PANGEA

Shuck B., H. Van Avendonk

The Eastern North American Margin (ENAM) formed in the early Jurassic (~195 Ma) after the breakup of supercontinent Pangea. This rifting event was accompanied by volcanism along the continental shelf of the eastern United States, giving rise to the East Coast Magnetic Anomaly (ECMA). Numerical models show that magmatic dikeing can assist rifting by reducing the effective stress required to rupture the lithosphere. Therefore, rifts with sufficient magma supply and extensional forces can develop a rapid transition from continental breakup to seafloor spreading. However, it is currently not well established whether the pace of breakup may be controlled by the arrival of mantle melts, or by thermal weakening and erosion of the lithosphere. Here we present analyses of active-source wide-angle seismic data collected during the 2014 ENAM Community Seismic Experiment in an area that extends farther offshore than previous seismic surveys along the eastern U.S. We find seaward of the ECMA lies a zone of thin oceanic crust with high compressional seismic velocity (up to 7.5 km/s in the lower crust), whereas thicker oceanic crust lies ~200 km farther offshore along another prominent magnetic anomaly, the Blake Spur Magnetic Anomaly (BSMA). We reconcile our seismic images with a petrologic model to evaluate the mantle melting conditions during the late stages of continental breakup and early seafloor spreading in the Central Atlantic. We find that the zone of thin crust between the ECMA and BSMA with high seismic velocity lower crust is best explained by the presence of a 17-21 km thick lithospheric lid which increased the average depth of melting and limited the amount of mantle melting. Our analysis suggests that the volcanism that produced the nearshore ECMA did not lead to complete breakup of the conjugate North American and African margins. Instead, normal seafloor spreading began at the BSMA under a moderate mantle potential temperature of ~1390-1415 C, ~25 million years after the initial formation of the volcanic margin. The mechanisms for continental breakup at the ENAM may be similar to the Afar region, where extension is accommodated by volcanic dikeing, however the lithosphere is still ~50 km thick.

EPISODIC HEATING OF CONTINENTAL LOWER CRUST DURING RIFTING

Smye A., L.L. Lavier, T. Zack, D.F. Stockli

Rheology of the continental lower crust plays an integral role in governing the style of continental extension. Creep deformation in the lower crust decreases lithospheric strength and promotes coupling of deformation in the brittle crust and upper mantle. Here, we present a high-temperature thermochronological investigation of the Ivrea-Verbano Zone-archetypal continental lower crust that was attenuated during opening of the Alpine Tethys oceanic basin. Rutile U-Pb dates and trace element concentrations, combined with thermal-kinematic modeling, show that the base of the Ivrea-Verbano Zone experienced heating on two timescales: conductive heating over $\sim 10^7$ yr, associated with thinning of the lithospheric mantle, and advective heating over $< 10^5$ yr, associated with high-temperature infiltration of fluids during crustal exhumation. These constraints match the thermal predictions of geodynamic models that predict high-magnitude thinning of lithospheric mantle during the early stages of extension. Conductive heating of lower crust directly preceded mantle exhumation and crustal excision, suggesting that thermal weakening of the lithosphere promotes focusing of extensional strain. Further, the thermal history of the Ivrea-Verbano Zone provides an example of the magnitude of heating that can occur during deep crustal extension; this has important implications for the genesis of granulite facies metamorphic rocks.

TOWARDS QUANTIFYING PLUME-LITHOSPHERE INTERACTIONS FROM GNSS GEODESY, SEISMOLOGY, AND GEODYNAMIC MODELING

Stamps D.S., A. Nyblade, E. Njinju, C. Bressers, G. Kianji, F. Tugume

We present an update on the GeoPRISMS project "Quantifying Plume-Lithosphere Interactions from GNSS Geodesy, Seismology, and Geodynamic Modeling". A 10 GNSS continuous station profile is deployed across the Eastern Branch and 9 broadband seismometers were installed in northeastern Uganda. By combining the existing GNSS data with our new observations and using constraints from the seismic data, we aim to (1) quantify strain accommodation across the Eastern Branch, (2) address the lack of resolution in existing upper mantle body wave tomography models and lack of seismic anisotropy beneath northern East Africa, and (3) develop a 3D geodynamic model of the lithosphere-asthenosphere system using products derived from the seismic data to test the role of plume-lithosphere interactions on surface deformation. Data from the seismic array are being added to an existing body-wave tomography model and have been used to develop seismic anisotropy observations. We have also developed a 3D regional model that is constrained by seismic tomography, lithospheric thickness, and includes weaknesses in the lithosphere. At this early stage in the project, we present our preliminary results from seismology and geodynamic modeling. The seismic data suggest the presence of NNE-SSW oriented seismic anisotropy and low wave-speed anomalies beneath the Kenya Rift, mainly to the south of Lake Turkana, and a craton-like fast-wave speed anomaly under the Ugandan Basement Complex. We also find that edge-driven convection may drive northward flow along the Eastern Branch towards the Afar.

STUDYING THE COUPLING BETWEEN DEFORMATION, PORE PRESSURE, AND FLUID FLOW IN SUBDUCTION FOREARCS

Sun T., D. Saffer, S. Ellis

The forearc portion of a subduction zone is among the most mechanically and hydrologically active tectonic settings. Here, porous and fluid-rich sediments on the incoming plate are either underthrust with the lower plate or off-scraped and accreted into the frontal part of the subduction wedge. The accompanying mechanical loading, as the sediments are subjected to increasing overburden and lateral tectonic compression, leads to porosity reduction (consolidation) and elevated pore pressure, which drives subsequent fluid drainage, with the flow rate controlled by the permeability of the system. Fluid pressure, in turn, affects the mechanical behavior of the sediments and fault zones and may affect the occurrence or propagation of earthquake rupture and slow slip. We employ the Lagrangian-Eulerian finite element code SULEC to quantitatively investigate these coupled processes. Using laboratory experimental results and field observations as constraints, we define fundamental relations between key physical properties associated with loading and drainage processes. Our model that covers the most seaward 40 km of the subduction wedge demonstrates the coupled evolution of deformation (strain and stress), pore pressure, and fluid flow toward building a tapered subduction wedge. Effects of various geological and hydraulic factors, including roughness of the plate interface, are rigorously tested.

ALONG-STRIKE VARIATIONS IN PROTOTHURST ZONE CHARACTERISTICS AT THE NANKAI TROUGH SUBDUCTION MARGIN

Tilley H., G.F. Moore, M. Yamashita, S. Kodaira

Protothrust zones (PTZs) are assumed to control the development of new frontal thrusts at subduction zones. PTZs are areas of incipient thrust faulting between the deformation front and the frontal thrust. However, limited resolution of previous seismic studies has hindered the study of their role in subduction accretion. New high-resolution seismic reflection surveys enabled detailed analysis of the PTZ along the Nankai Trough, SE Japan. Seventeen multichannel seismic reflection lines were collected perpendicular to the trench axis between Cape Ashizuri and Cape Muroto using a 1200 m long, 192 channel hydrophone cable and a 380 in³ (5.24L) cluster airgun array. These lines were processed using pre-stack depth migration. PTZs only existed where a turbidite sequence was present beneath the trench wedge. The PTZs consisted of closely spaced, sub-parallel protothrusts that decreased in spacing and increased in length landward. Where the turbidites were truncated by basement topography, there was a transitional PTZ heterogeneous protothrusts and small displacement thrust faults. We hypothesize that elevated pore pressures due to the low permeability hemipelagic sediment inhibit the formation of PTZs and favor small displacement thrusts in a narrow trench wedge. Conversely, turbidite layers within the hemipelagic sediment allow drainage and reduce the pore pressure. This increases the effective stress and shear strength on faults, resulting in strain localizing protothrusts. This implies that the changes in pore pressure imposed by differences in the sediment permeability control the style of deformation in the trench wedge and consequently, the geometry of the accretionary wedge.

THE SZ4D VISION: PLANNING FOR AN INTEGRATED SUBDUCTION RESEARCH PROGRAM

Tobin H. and the SZ4D RCN Steering Committee

SZ4D, or Subduction Zones in Space and Time, is a community-based initiative to investigate the fundamental processes underlying the hazards related to subduction. Following the publication of the SZ4D Vision Document, effort has advanced on multiple fronts to turn that vision into concrete plans. NSF has now funded three RCNs (Research Coordination Networks) to explicitly support communication and planning for a decadal-scale, broad-based effort by the scientific community to research processes ranging from megathrust and upper plate seismic locking and release in earthquakes to surface instability leading to landslides and lahars, and to the magmatic processes driving volcanic eruption. The SZ4D "Umbrella" RCN will coordinate these efforts and develop viable long-term research strategies and plans for observational and intellectual infrastructure to make it happen. The aim is for a program that represents community consensus on where US subduction research may focus in the post-GeoPRISMS, post-Earthscope era. This poster will provide information on how interested researchers at all career stages can get involved in that planning.

FROM SOURCE TO SINK: TECTONIC-LANDSCAPE EVOLUTION MODELING OF A CONTINENTAL RIFT


van Wijk J., M. Berry

We use a tectonic-landscape evolution model to study sediment infill of an opening rift basin. In the model, extension results in opening of an asymmetric half-graben along a listric normal fault. Rift opening occurs in wet, temperate, or semi-arid climates. We performed a sensitivity analysis to explore the effects of tectonic parameters such as rift-opening rate, and model parameters such as sediment transport capacity and antecedent drainages on landscape evolution and endorheic-exorheic transitions. Our numerical experiments show that slow rift-opening rates, a slowing-down of rift opening, or increase of headwater topography (e.g., upstream epeirogenic uplift), are tectonic situations that can cause a transition from an endorheic (internally drained) to an exorheic (externally drained) drainage state in a rift basin. Our results also show that wet climate conditions lead to a permanent exorheism that persists regardless of rift opening rates. In semi-arid climates, endorheic conditions are favored, and may last for the duration of rifting except for when rift opening is very slow. Our results form an interpretive framework to study endorheic and exorheic drainage systems in natural continental rifts.

NEOGENE STRESS ROTATION AT THE TRANSITION FROM SUBDUCTION TO CONTINENTAL COLLISION, MARLBOROUGH, NEW ZEALAND

Willis D., P. Betts, L. Moresi, L. Ailleres

The convergent plate boundary between Australian and Pacific Plates in the SW Pacific transitions from unimpeded subduction to subduction impeded by the oceanic Hikurangi Plateau and through to continental collision. The Marlborough Fault Zone forms the structural link between asymmetric rollback along the Tonga-Kermadec-Hikurangi Subduction Zone and oblique dextral-reverse continental collision along the Alpine Fault. Using numerical models of subduction we show that asymmetric rollback is driven by subduction of the Hikurangi Plateau, causing a rotation in the stress field along the plate boundary. Paleo-stress inversion of striations recorded on faults within the Marlborough Fault Zone display a rotation of stress field from 69°N to 116°N, at a rate of ~7°/Ma since 7 Ma. This rotation in stress field has transitioned the slip on the NE striking faults from dextral strike-slip to dextral reverse, increasing the shortening component accommodated during deformation.



Scientists check out the active fumarolic fissure at the summit of Kanaga Volcano on September 22, 2015. The "NSF GeoPRISMS Shared Platform R/V Maritime Maid Leg 3: Western Aleutians" facilitated the team's expedition to seven active volcanic islands, from Kanaga to Buldir, in search of mafic tephra. Photo credit: E. Cottrell

VOLATILE CONTENTS OF WESTERN ALEUTIAN MAGMAS AND THEIR RELATIONSHIP TO SLAB THERMAL STRUCTURE

Andrys J., K. Kelley, E. Cottrell, M. Coombs

The Aleutian arc transitions from normal convergence in the east to oblique convergence in the west. Several studies predict that this, coupled with the prospect of a torn slab edge, should cause the slab to be both hotter and drier in the west. Increased slab temperature can cause premature devolatilization of the slab beneath the forearc, leaving fewer volatiles to flux into the arc magma source. We assessed H₂O by FTIR and sulfur by electron microprobe in olivine-hosted melt inclusions from 5 volcanoes in the western Aleutians. We observe an along strike trend of increasing H₂O from east to west across the arc with a max water content of 6.76 wt% occurring at Buldir, the furthest west emergent volcano. We observe no along strike trend in sulfur or H₂O/Ce ratios, a common proxy for slab surface temperature. This scenario of highly hydrous magmas generating from a hot slab setting could be explained if water were coming from a hydrated slab mantle rather than the slab surface. Fluids coming from a hydrated slab mantle would not be saturated in monazite or allanite as is required to apply the H₂O/Ce method for slab temperature, thus explaining the disagreement between H₂O/Ce and geophysical models. To achieve dehydration of the slab mantle, the western Aleutian slab would need to be hotter than current geophysical models predict.

FROM AOC TO ECLOGITE: HALOGEN BEHAVIOR DURING DEVOLATILIZATION IN THE FOREARC

Beaudoin G., J. Barnes, T. John

During hydrothermal alteration on the seafloor, ocean crust becomes enriched in halogens. When this altered ocean crust is subducted, it undergoes metamorphism and devolatilization. The addition of halogens during geologic processes alters fluid properties, phase stability, and element solubility. However, the abundances and behaviors of halogens in altered oceanic is not well constrained. In this project, eclogites from three paleo-subduction settings have been compared to modern oceanic crust in an effort to observe large-scale changes that occur during prograde subduction. Results indicate that F and Cl are decoupled during prograde metamorphism. F demonstrates immobile behavior, preserving near-protolith concentrations up to eclogite facies. Alternatively, Cl exhibits fluid-mobile behavior and is generally lost from the slab during prior to reaching eclogite facies. Despite the loss of Cl, the Cl stable isotope compositions do not appear to fractionate with devolatilization. The distinct behaviors of F and Cl within subducting altered oceanic crust suggests differing mineralogical and local controls, providing the impetus for future research which explores in situ variations in halogen concentration.

GEOCHEMICALLY CONSTRAINING THE DEPTH OF THE LITHOSPHERE-ASTHENOSPHERE BOUNDARY IN THE CENTRAL MAIN ETHIOPIAN RIFT SYSTEM

Chiasera B., T.O. Rooney, I. Bastow, G. Yirgu, E. Grosfils, D. Ayalew, P. Mohr, J. Zimbelman, M. Ramsey

Lithospheric thinning and melt generation are recognized as being integral to continental rifting. Geochemical estimates of the shallowing of the lithosphere-asthenosphere boundary (LAB) have largely been based on quantitative evidence (e.g. xenolith thermobarometry), isolated from determinations of melt ascent pathways through the asthenosphere. The Galema range, an area of focused magmatic activity along the eastern margin of the Central Main Ethiopian Rift, provides an opportunity to examine the impact of extension on lithospheric thickness. We present whole-rock trace element data on 77 samples of magmatic products of the Galema range, and high precision olivine chemistry on 52 crystals from 5 samples. Models constraining melt generation conditions within the source of the magmas reveal that they were generated at 1419-1450°C and at 103-114 km. depth. These results contrast with thermobarometric calculations of where such magmas stalled and last re-equilibrated with the mantle. Si/Mg activity thermobarometry determined this temperature to be 1435-1474°C and depth to be 78-89 km. We contend that this depth of stalling represents a thermochemical boundary to ascent, defined as the LAB, which exists at ~80km. depth locally. These results indicate the lithosphere has been thinned in response to continental rifting processes affecting the African continent.

BUILDING ARC CRUST – PLUTONIC TO VOLCANIC CONNECTIONS IN AN EXTENSIONAL OCEANIC ARC, THE ALISITOS ARC CRUSTAL SECTION (SOUTHERN ROSARIO SEGMENT), BAJA CALIFORNIA

Morris R., S.M. DeBari (presenter), C. Busby, S. Medynski

The ~60 km long Rosario segment of the Cretaceous Alisitos arc terrane provides undeformed 3-D exposures of the upper 7 km of an oceanic extensional arc, where crustal generation processes are recorded in the both the volcanic and underlying plutonic rocks. These exceptional exposures allow interpretation of the differentiation processes active during the growth and evolution of the arc crust.

Upper crustal rocks in the Rosario segment consist of a 3-5 km thick volcanic section with hypabyssal intrusions. Plutons intrude these units at various levels along strike, but at each intrusive contact the transition is complete over a distance of <150 m, where stoped volcanic blocks are present. There is striking compositional overlap in whole-rock and mineral chemistry between the plutonic and volcanic units, suggesting a comagmatic source. Units are predominantly low-K with flat REE patterns, and show LILE enrichment and HFSE depletion. Initial isotope ratios (Sr, Nd, Pb) overlap for all units and imply no cratonic continental involvement. This agrees with low Sr/Y ratios of all rock types, indicative of thin, immature oceanic arc crust.

Modeling results show that closed-system fractional crystallization drove crustal differentiation from mafic to intermediate compositions, but open-system processes likely occurred to produce some of the felsic compositions. Our results can be used as a reference model for differentiation processes relating to the growth of the middle and upper crust within active extensional arc systems. The Rosario segment plutonic rocks may be analogous to the low-velocity zone ($V_p=6.0-6.5$ km/s) imaged within arcs worldwide.

RECONTEXTUALIZATION OF ACROSS-ARC SIGNATURES IN THE IZU BONIN ARC, LINKING MAFIC TO FELSIC MAGMATISM ACROSS THE ARC

Heywood L.J., S.M. DeBari (presenter), S.M. Straub, J.B. Gill, J.C. Schindlbeck, D.R Escobar

Izu Bonin rear arc tephras (1.1-4.4 Ma) from IODP Site U1437 provide a well-dated record of changing magmatic compositions during the timespan when the Izu-Bonin arc began its most recent episode of rifting. Considered with a comprehensive recontextualization of published analyses of <7 Ma regional dredged rocks, magmatic compositions are shown to vary in coherent chronological and spatial trends and can be classified into three series: LREE-depleted volcanic front series; flat pattern REE rift-related series; and LREE-enriched rear-arc seamount chain-type (RASC-type) series which includes Site U1437 glasses. Each series has a distinctive characteristic basalt type whose trace element and radiogenic isotope chemistry matches rhyolite type from the same region. RASC-type magmatism is shown to extend to younger ages than previously reported.

INSIGHTS INTO THE ARCHITECTURE OF ACTIVE CONTINENTAL ARCS FROM GEOCHEMICAL AND SEISMIC DATA

Delph J., K. Shimizu, B. Ratschbacher, D. Rasmussen, X. Pu

The chemical differentiation mechanisms and storage depths of primitive, mantle-derived magmas to more silicic compositions in active arc systems is still debated and requires the integration of geochemical and seismic observations. Geochemistry can estimate the pressure-temperature stability conditions of phases through geobarometry and thus the depth ranges of magmatic storage and crystallization, whereas geophysical techniques, such as seismic velocity imaging, can offer a more complete understanding of the presence and depth distribution of melt in an active magmatic system. However, seismic velocities are non-unique with respect to composition and melt content, and cannot “image” geochemical processes such as magmatic differentiation. Therefore, we combine seismological observations with geochemical data of recent eruption products at an active lithospheric-scale magma plumbing system in the southern Puna Plateau to better constrain the present-day magmatic architecture of a continental arc system.

Our results reveal that magma stalling and compositional differentiation is occurring predominantly at two locations: 1) near the base of the crust, where seismic velocities are anomalously slow (1.2 GPa) and fractional crystallization alongside assimilation of crustal material, and 2) in a mid-crustal reservoir beneath the Cerro Galan Caldera, where shear-wave velocities necessitate the presence of melt (~2.7 km/s) and negative Eu anomalies show evidence of low-pressure differentiation processes. Thus, our combined geophysical and geochemical investigation indicate a presently active, multi-level crustal magma plumbing system beneath the Southern Puna Plateau, in which magma stalls and differentiates preferable at the crust-mantle boundary and in the mid-crust.

EVALUATING THE ORIGIN OF PYROXENITE XENOLITHS IN THE EAST AFRICAN RIFT SYSTEM VIA RE-OS ISOTOPES AND HIGHLY-SIDEROPHILE ELEMENTS

Ducatte A., W.R. Nelson, E. Pitcavage, E. Barijaijo, P. Kalegga Kulyanyingi, T. Furman

Pyroxenite is the dominant lithology of xenoliths brought to the surface via recent volcanism in the Uganda region of the East Africa Rift System (EARS). This lithology is unique compared to most xenoliths found in the Ethiopian and Tanzanian portions of the EARS. To understand the origin of the pyroxenites, Re-Os isotopes and highly siderophile element (HSE) abundances were measured on 21 xenoliths from the Bufumbira (Virunga) volcanic province in the Western Rift. The majority of Bufumbira pyroxenite xenoliths have a range of Os isotopes that were moderately to highly enriched in $^{187}\text{Os}/^{188}\text{Os}$ (0.1329-0.5743) compared to primitive mantle (0.1296). Samples from Bufumbira site 02 displayed much higher concentrations of Re (1.5-2.0 ppb) than other sites (0.023-0.490 ppb). Chondrite-normalized HSE patterns are consistent with melt fractionation. Most Bufumbira xenoliths record $\text{Ir}/\text{Ru} = 1.69\text{-}9.50$ while some record more extreme values ($\text{Ir}/\text{Ru} = 0.13$ and 25.41). Similarly, Os/Ru ratios range from 0.749-6.02 across all sites with three samples exceeding 10. Compared to primitive mantle ($\text{Ir}/\text{Ru} = 0.50$ and $\text{Os}/\text{Ru} = 0.56$), most of the xenoliths have a Ru depletion. Apart from several samples from different sites with high values (12.25-54.90), Ir/Re ratios were from 0.002 to 3.30. The moderately to highly fractionated chondrite-normalized HSE patterns with large Ru depletions are indicative of a melt-dominated system, meaning the HSE signature was inherited from the melt passing through and interacting with the mantle to generate the pyroxenites. East Africa was assembled during the late-Proterozoic Pan-African Orogeny, making subduction a plausible origin for the pyroxenite xenoliths.

USING MAGMA DYNAMICS MODELS TO INTEGRATE GEOCHEMICAL AND GEOPHYSICAL DATA IN A PROCESS- BASED FRAMEWORK

Dufek J., G. Eggers, N. Andersen

The assembly of large silicic magmatic centers encompasses processes that span many time and length scales from the initial processes of mantle melting and extraction, to the transport, interaction, differentiation, and residence in the crust. These magmatic systems are coupled to their crustal containers, exchanging mass and energy, and responding to evolving tectonic conditions and crustal lithologies. In this work, we use multiscale numerical models in conjunction with recent information from the on-going geophysical and geochemical investigation of one large silicic center, Laguna del Maule (Chile), to examine the response of the crust to sustained input of magmas from the mantle. The Laguna del Maule (LdM) volcanic field in Chile has been one of the most active rhyolitic centers following deglaciation, and this part of the arc has likely been continuously active for ~25 MY (Hildreth et al, 2010).

We use a 3D multiphase model to examine the evolution of the Laguna del Maule system and explore the magmatic flux that is consistent with a range of observations. This model simultaneously calculates heat transfer, melt dynamics, and phase equilibria. We particularly focus of the long-term history of magma in the crust including melt residence and spatio-temporal relationship of melt in the crust.

NEW CONSTRAINTS ON THE EAST AFRICAN RIFT FROM AXIS TO FLANK USING A COMBINATION OF SEISMIC DATA TYPES

Eilon Z., J. Petruska, K. Keranen

The Main Ethiopian Rift is the most highly-extended portion of the East African Rift, the global archetype for active continental divergence. New broadband seismic data extends high-quality coverage of this rifting margin from the rift axis to its flank, offering - for the first time - the opportunity to understand active rifting in the full context of pre-existing continental structure. We couple surface wave phase velocity measurements with body wave scattered phase data to image the detailed deep structure of this region from axis to flank. We interpret this data together with new measurements of teleseismic body wave attenuation, and work towards a synthetic understanding of the temperature, crustal thickness, presence and distribution of melt, and lithospheric structure across this complex system.

SEISMIC LAYER 2A: EVOLUTION AND THICKNESS FROM 0-70 MA CRUST IN THE SLOW-INTERMEDIATE SPREADING SOUTH ATLANTIC

Estep J., B. Reece, D. Kardell, G. Christeson, R. Carlson

Layer 2A, the porous and permeable uppermost igneous oceanic crust, permits the circulation of fluid within the crust, the exchange of dissolved mineral species between the ocean and crust, and the convective dissipation of heat from the crust. We examine the presence, temporal extent, thickness, and evolution of layer 2A using multichannel seismic data collected at 30°S in the South Atlantic across crustal age ranges of 0-70 Ma and half spreading rates of 12-31 mm/yr. We observe that the layer 2A/2B boundary is present in 0-48 m.y. old crust, but not in crust older than ~48 Ma. The thickness of Layer 2A in the South Atlantic has substantial variability, with a mean of 760 m and a standard deviation of 290 m. Layer 2A has no systematic change in thickness with age in the South Atlantic and thickness does not correlate with spreading rate. The crust in the South Atlantic is never fully sealed by sediment cover, which implies that the fluid circulation system in the upper crust never becomes fully closed and the thickness of layer 2A can work as a proxy for the depth at which significant circulation can occur. The disappearance of the layer 2A/2B boundary in older crust implies that fluid circulation within the upper crust continues to occur for at least ~48 m.y. after crustal formation in the South Atlantic, after which layer 2A becomes indistinguishable from layer 2B based on velocity gradients.

EFFECT OF THERMALLY-CONTROLLED PERMEABILITY BARRIERS ON THE LOCATION OF ARC VOLCANISM AT SUBDUCTION ZONES

Ha G., L. Montesi, W. Zhu

It is generally believed that slab dehydration at subduction zones occurs at a critical depth around 100 km that promotes melting and magmas move vertically due to the buoyancy. However, observations show that slab depth is actually very variable while having a norm at 100 km. We examine here the alternative hypothesis that arc location is controlled by the thermal structure of the overriding plate, specifically the location and shape of a thermally-controlled permeability barrier in the upper plate. The arc may be located at the apex of the permeability barrier or where the barrier intersects the base of the overriding crust, regardless of the original location of melting. To test this idea, we compare the arc locations predicted in our models to the actual arc locations at 16 subduction zones. For 13 subduction zones, dehydration depth and the apex of isotherms can explain the observed arc location, but for three subduction zones, both predictions cannot explain the arc location. We couldn't find any systematic relation with other subduction parameters that can affect the prediction, such as slab parameter, dip and the type of overriding plate, the results show that it is conceivable that arc location is controlled by the thermal structure of the overriding plate and not the depth of slab dehydration, motivating us to study a broader selection of subduction zones.

BILLION-YEAR STABILITY OF CRATONIC EDGES CONTROLS LOCATION OF GLOBAL SEDIMENT-HOSTED METALS

Hoggard M., K. Czarnota, F. Richards, D. Huston, L. Jaques

Consumption of base metals (copper, lead, zinc and nickel) over the next ~25 years is set to exceed the total produced in human history to date. Major factors driving this demand are global development and the transition to clean energy sources. Moreover, trace metals that are essential to high-tech applications (e.g. cobalt, indium and germanium) are often produced as by-products of base metal mining. A growing concern is that the rate of exploitation of existing reserves is outstripping discovery of new deposits, despite exploration expenditure tripling during the 2005-2012 minerals boom. Improvements in the effectiveness of exploration for mineral deposits, particularly those buried under shallow cover, are required to reverse this worrying trend and maintain growth in global living standards. Here, for the first time, we show that giant sediment-hosted base-metal deposits occur exclusively along the edges of thick lithosphere. ~90% of the world's sediment-hosted copper, lead and zinc resources lie within 200 km of these boundaries. This result provides an unprecedented global means to identify fertile regions for targeted mineral exploration, reducing the search-space for new deposits by approximately two thirds on this criterion alone. In addition to these exploration implications, the 2-billion year age range of these deposits indicates that edges of thick lithosphere are mostly stable over this time period without appreciable thermo mechanical erosion.

LOW-SALINITY FLUIDS IN AN INTRA-SLAB SHEAR ZONE: INSIGHTS INTO FLUID SALINITY FROM APATITE IN THE MONVISO OPHIOLITE (WESTERN ALPS)

Hoover W., S. Penniston-Dorland, P. Piccoli

Apatite offers a unique perspective on fluid composition in high-pressure metamorphic rocks because of its ability to incorporate halogens, which can dramatically affect the fluid mobility of many metals. Here we present halogen and major element compositions of apatite from the Monviso Ophiolite (Western Alps, Italy) to explore fluid salinity, and the fluid flux transported by an apatite vein. Apatite in Monviso is fluorine-poor (only 23 to 37% fluorapatite) compared to other high-pressure (HP) metamorphic apatite but has typically low chlorine concentrations (<2.2 wt% Cl). The salinity of fluids in equilibrium with our apatites were calculated to contain 0.9 to 4 wt% NaCleq based on apatite-fluid Cl partitioning experiments. These values are comparable to fluids released by dehydration of the subducting slab (0.25 to 8 wt% NaCleq), but lower than other estimates from the Monviso Ophiolite (5 to 20 wt% NaCleq). One sample contains apatite in a monomineralic vein formed near peak metamorphism. The fluid flux necessary to produce this vein was calculated using experimentally-derived solubilities of apatite in H₂O and H₂O+NaCl fluids yielding fluxes of 10⁸ and 10⁷ m³/m², respectively. These results are one to two orders of magnitude higher than any other metamorphic setting worldwide suggesting either the natural fluid was markedly different from those used in the solubility experiments, or precipitation was driven by changes in fluid chemistry not accounted for in our model. Differences in salinity estimates between textural settings in Monviso could record multiple fluid compositions and warrant further investigation.

POTENTIAL CAUSES OF CRYSTAL-MELT DISEQUILIBRIUM IN KARISIMBI LAVA

Ishimwe F., T. Rooney, A. Steiner

Potassic alkaline magmatism is uncommon, occurring mainly within intracontinental extensional tectonic environments. The high concentration of alkalis in these lavas is thought to be related to either the low degree of melting in the upper mantle, or melts derived from metasomatized mantle. However, uncertainty persists as to the mantle generation and evolution processes of these alkali-rich lavas. There is thus a compelling need to examine the mechanisms by which potassic magmas evolve. The western branch of the East African Rift provides among the best examples of a potassic magmatic province. Within the western branch of the East African Rift the Virunga Volcanic province is comprised of eight volcanoes. Here we examine the magmatic evolution of Karisimbi, the largest volcano in this magmatic province using petrographic and geochemical techniques. Trace elements of newly recovered samples show enrichment in LIL elements while showing negative phosphorus and titanium anomalies in evolved lavas. These observations agree with major elements trends suggesting that fractional crystallization played a large role in Karisimbi magmatic evolution. However, presence of resorbed biotite, zoned plagioclase, and potassium feldspar xenocrysts evidence more complicated magmatic process within this volcano's magmatic plumbing system. This study probes other factors contributing to Karisimbi's evolution.

PYROCLAST TRANSPORT DYNAMICS DURING THE 2012 ERUPTION OF HAVRE VOLCANO (KERMADEC ARC)

Jones, M.R., S.A Soule, A. Woods, K.E. Fauria, R. Carey, J.T. Perron, M. Manga

More than 70% of the Earth's volcanic output happens underwater. However, the hazards posed by submarine silicic eruptions are relatively poorly understood, partially due to limited observations from these remote settings. In July 2012, the discovery of a large pumice raft floating between Tonga and Auckland spurred an exceptionally thorough exploration of the eruptive products from a submarine silicic eruption. Moderate-Resolution Imaging Spectroradiometer (MODIS) images elucidated the production and dispersal of a 400-km² pumice raft (Jutzeler et al., 2014). A comprehensive 1-m resolution bathymetric map produced by the autonomous underwater vehicle (AUV) Sentry along with 250 hours of video and 290 samples collected by the remotely operated vehicle (ROV) Jason illuminated new lava flows and domes produced from 14 vents, along with giant pumice blocks spread across the caldera (Carey et al., 2018). The distribution of giant pumice blocks provides new insight into submarine fragmentation processes and pyroclast transport and deposition.

STRUCTURE OF UPPER OCEANIC CRUST IN THE WESTERN SOUTH ATLANTIC USING FULL-WAVEFORM VELOCITY MODELING

Kardell D., G.L. Christeson, R.S. Reece

The upper oceanic crust is extremely difficult to image using conventional seismic imaging methods due to its complex internal structure and scattering of seismic energy on rough seafloor or basement topography diminishing the signal-to-noise ratio. Recent advances in seismic data processing allow us to build high-resolution velocity models of the upper oceanic crust that can provide us with clues on physical properties and seismic structure. We perform full-waveform inversion of long-offset streamer data to explore the seismic velocity structure at the Mid-Atlantic Ridge (MAR) and faulting both on and off-axis. The results will build upon previous work revealing the regional seismic velocity distribution of upper oceanic crust between the MAR and the Rio Grande Rise. Two important issues that will be addressed are the nature of the seismic layer 2A/2B boundary and the inferred geometry of hydrothermal circulation.

THE INITIATION OF VOLCANIC ERUPTIONS

Kent, A., C. Till, K. Cooper

A key source of information regarding volcanic eruptions are the set of processes that lead from storage of magma in a stable or quasi stable mode in the shallow crust, to movement of magma upward, eventually to breach the surface and cause an eruption. We describe this as eruption initiation. An understanding of the key physical and chemical processes that lead to eruption initiation are important for considering hazards and responses associated with future eruptions, for resurrecting the past behavior of volcanic systems from the geological record, and for correctly interpreting monitoring and other data which allow us to anticipate future and ongoing volcanic behavior. Although there is surprisingly little published literature dedicated to understanding eruption initiation, petrological approaches are particularly amenable to studying initiation in both modern and prehistoric eruptions. Initiation typically involves some of the last high temperature processes that affect erupted magmas, and these often leave clear signals preserved in the petrographic record. Petrological techniques are also increasingly providing access to the timescales of eruption initiation, which are important for evaluating future volcanic hazards.

We present a survey of eruption initiation mechanisms deduced from petrology and other observations for selected volcanoes of the Cascade arc. A number of different mechanisms are evident, related to magma recharge, magma mixing, and vapor accumulation or second boiling. Timescales associated with initiation, including the time between recognition of volcanic unrest via seismic, gas or other remote means, and the time at which magma breaches the surface, appear to range between weeks and months.

HOW DOES DIFFUSE CO₂ FLUX VARY ACROSS THE EAST AFRICAN RIFT SYSTEM?

Muirhead J., T. Fischer, A. Laizer, A. Zafu, H. Lee, S. Oliva, R. Pik, B. Marty, E. Judd, E. Kazimoto, M. Broadley, G. Kianji, D. Ayalew, A. Caracausi, C. Ebinger

Magma-rich continental rifts represent a key tectonic setting for natural CO₂ emissions into Earth's atmosphere, and possibly modulate Earth's climate on geological timescales. However, the total volume of mantle CO₂ emitted at rift settings is poorly constrained, as well as the mechanism that control variations in CO₂ flux over the lifetime of rifting. We examined diffuse CO₂ emissions at various settings along the magma-rich Eastern Branch of the East Africa Rift System (EARS) using the soil CO₂ accumulation chamber method. The purpose of this study is to test how mantle CO₂ fluxes vary as a function of initial lithospheric conditions, magmatic-volcanic outputs, and the stage of rift evolution. Our results suggest that the volume of diffusely emitted mantle CO₂ at rift settings is dependent on the nature of the carbon source and total magma production. In settings with higher rates of magmatism/volcanism (i.e., Afar Depression, Ethiopia, and Magadi basin, Kenya), greater CO₂ outputs are observed in rift basins that have undergone less stretching, and are hence underlain by a greater volume of subcontinental lithospheric mantle. For early-stage basins (e.g., Natron, Manyara, and Balangida basins of Tanzania), mantle CO₂ fluxes reduce as the EARS crosses from the Proterozoic Mobile Belt to the Tanzanian Craton. This suggest that mantle CO₂ flux in the EARS is also dependent on the nature of the initial rifted lithosphere (e.g., craton vs mobile belt). We conclude that annual estimates of mantle CO₂ emissions from continental rift systems must not only consider magma production rates, but also the state of the initial cratonic lithosphere and the volume of subcontinental lithospheric mantle underlying the rift system. Many of these conditions will vary over the course of rift evolution.

THE ROLE OF SLAB MELTS IN THE SULFUR CONTENT, METAL CONTENT, AND OXIDATION STATE OF PRIMITIVE ARC MAGMAS IN THE SOUTHERN CASCADES

Muth M., P.J. Wallace, K.J. Walowski

Arc magmas are oxidized relative to mid-ocean ridge basalts, but the causes of this oxidized signature are uncertain. This study uses primitive olivine-hosted melt inclusions from the tephra of basaltic cinder cones in the Southern Cascades to investigate the role of slab-derived sulfur in the oxidation state, sulfur content, and chalcophile element behavior of primitive arc magmas. We integrate evidence for a hydrous slab component in Lassen primitive magmas from previous work with evidence from major element, trace element, and chalcophile element concentrations in addition to fO_2 values from XANES analysis. fO_2 values for the different cinder cones correlate with S/Dy and Sr/Nd values and are consistent with the addition of oxidized, sulfur-carrying slab material to the Lassen sub-arc mantle. Cu/Sc values approach average MORB values and are similar between cinder cones despite significant differences in fO_2 and sulfur concentrations. This suggests that chalcophile element behavior is moderated by the presence of a residual sulfide phase during melting within the Lassen sub-arc mantle.

MAGMA AND VOLATILE COMPOSITION OF SOUTH ISLAND, TURKANA

Owens M.G., T. Rooney, A. Steiner, B. Chiasera, P. Wallace

Lake Turkana, which represents the modern expression of extension in the East African Rift, is comprised of a series of half grabens and three recent volcanic islands. These islands define the modern axis of magmatism within the rift, which extends discontinuously from Afar in the north to Tanzania in the south. South Island, the largest of the three islands, is comprised of dominantly basaltic magmatism expressed as tuffs, scoria, and flows. Here we present a partial volcanic stratigraphy for the island and a geochemical characterization of the magmatic products. South Island represents an important insight into the melting conditions in the regional upper mantle as it contains more mafic basalts in comparison to the other islands. A critical unknown within studies of primitive melts in East Africa are constraints on the volatile content of rift magmas. We therefore present olivine-hosted melt inclusion volatile data from several samples from South Island. These data represent the first study of magma volatiles in the Turkana Depression, providing insight into both the volatile composition of the magma source, and depth of magma crystallization.

CROSSING THE GAP: LINKING THE EOCENE AND OLIGOCENE EAST AFRICAN RIFT VOLCANICS

Peterson L., T. Rooney, A. Steiner, J. Kappelman

The Ethiopian Large Igneous Province was produced by the interaction of thermo-chemical plume(s) and extensional plate-tectonic processes. Geochemical and petrological studies have revealed two pulses of magmatism, the first in southern Ethiopia during the Eocene, and the second in northwestern Ethiopia during the Oligocene. The Makonnen basalts in S. Ethiopia, which exhibit a stratigraphic thickness of 700 m, are temporally bound by Eocene and Oligocene volcanics. The spatial separation between these events has complicated efforts to understand the relationship between the pulses. Despite the important link that these lavas represent, the relationship between the Makonnen, Eocene, and Oligocene events remains unknown. Here we present a new geochemical dataset from the Makonnen type sections, using sample fragments collected by a joint expedition of the Ethiopian Government and the Canadian Geological Survey in the 1970s. Preliminary results demonstrate that the Makonnen basalts differ from the Oligocene magma types. Instead, these basalts closely resemble those of the Eocene Gamo lava pulse. The implications of this observation are that the source of the Eocene basaltic pulse is more extensive both spatially and temporally. We discuss these results in the context of the dual pulse plume model and the northward movement of the African plate.

SPATIAL DISTRIBUTION OF THE AMARO AND GAMO BASALTS: GEOCHEMICAL ANALYSIS OF THE ROCKS OF THE OMO RIVER PROJECT

Phillips R., T. Rooney, A. Steiner, G. Girard, J. Kappelman

Magmatic activity in the East African Large Igneous Province (LIP) is characterized by pulsed eruptive events: (A) an initial Eocene phase (ca. 45 to 35 Ma) that is centred on Southern Ethiopia and, (B) a subsequent Oligocene phase (ca. 32-28 Ma) that is centred on the northwest Ethiopian Plateau. The Eocene phase has attracted little scientific attention, despite it representing about 20% of the entire LIP volume. Prior studies divided magmatism into a lower Amaro and upper Gamo lava series; however, these studies consisted of only three stratigraphic sections located along the margin of the Main Ethiopian Rift. To expand the geographic distribution of geochemical data of the older event, we present geochemical data for the Eocene basalts of the Omo region. These data expand the existing catalogue westward by ~150 km, allowing a probe into the spatial relationship between the distribution of Amaro and Gamo basalts. Major and trace element characterization of our Omo basalts reveal they are identical to the Gamo basalts. These results suggest that the older Amaro basalts may be limited in spatial extent, while the slightly younger Gamo basalts may be much more extensive than previously understood.

NEW OLIVINE-MELT Ni THERMOMETER FOR HYDROUS BASALTS AND ITS APPLICATION TO REVEAL VARIATIONS IN LITHOSPHERIC THICKNESS IN WESTERN MEXICO

Pu X., R. Lange, G. Moore

A new olivine-melt thermometer (Pu et al., 2017) based on the partitioning of Ni (D_{Ni}/liq) was hypothesized to have a negligible dependence on dissolved H_2O content in the melt at <1 GPa. To test this hypothesis, new olivine-melt equilibrium experiments were conducted on a basaltic glass under hydrous and anhydrous conditions. The Ni-thermometer recovers the T_{expt} for all the experiments within an average of $14^\circ C$, demonstrating that the olivine-melt thermometer based on D_{Ni}/liq can be applied to hydrous arc basalts at depths < 1 GPa without corrections for dissolved water in the melt (Pu et al., submitted).

This new olivine-melt Ni thermometer have been applied to a set of arc basalts/basaltic andesites from the Tancitaro Volcanic Field and a set mantle-derived K-rich minettes and absarokites from the Colima rift in Western Mexico to determine the temperature and minimum H_2O concentrations at the onset of olivine growth. From there, melt segregation depth for both sets of samples were also estimated based on mantle melting experimental results. The P,T constraints for the two sets of samples illustrate two lithospheric blocks with different thickness in Western Mexico, which has led to for the different dips in the subduction of Rivera and Cocos plates.

CRUSTAL FORMATION AND PLUME PULSING IN THE NORTH ATLANTIC OCEAN

Parnell-Turner R., N. White, T. Henstock, J. Maclennan, S. Jones, B. Murton

In the North Atlantic Ocean, hot material rises up within the Iceland plume from deep within Earth's mantle, forming a regional-scale pancake-shaped upwelling. A pattern of distinctive V-shaped ridges (VSRs) and troughs that are hundreds of kilometers long and tens of kilometers wide can be observed either side of the Reykjanes Ridge to the south of Iceland. These VSRs are thought to be generated by waxing and waning of the plume, but their precise origin is hotly debated. Using seismic reflection data collected with colleagues from the UK, we assessed competing hypotheses for their formation, and found that they are likely to be an indirect record of plume activity through time. Pulses of hot material appear to be generated every 3 to 8 Ma. As they spread beneath adjacent tectonic plates, these pulses cause an increase in melting, which leads to the accretion of crust that is up to 2 km thicker than normal.

$\delta^{18}\text{O}$ RECORDS IN QUARTZ FROM OKATAINA VOLCANO, NEW ZEALAND: INSIGHTS INTO THE EVOLUTION OF A LARGE AND DYNAMIC SILICIC SYSTEM

Sas M., N. Kawasaki, N. Sakamoto, P. Shane, G. Zellmer, H. Yurimoto

The Okataina Volcanic Centre (OVC) is one of only two dormant caldera-forming centres in the world's most recurrently active silicic volcanic region – the Taupo Volcanic Zone in New Zealand. There has been periodic volcanic activity at OVC for the last 600,000 years, including three caldera-forming events and tens of intra-caldera eruptions. Using SIMS, we investigated the $\delta^{18}\text{O}$ isotopic ratios of quartz from several silicic OVC pyroclastic deposits in order to understand how crustal and mantle inputs have varied over time, especially considering the complexity of the associated subduction margin. Deposits studied, and their average $\delta^{18}\text{O}$ values, currently include the oldest caldera-forming eruption (Utu, 0.56 My, $7.47 \pm 0.23\text{‰}$ 2SD), a dome-building event (Haparangi, ~200 ky, $7.08 \pm 0.25\text{‰}$ 2SD), the youngest caldera-forming eruption (Rotoiti, 45 ky, $7.67 \pm 0.23\text{‰}$ 2SD), and two recent eruptions (Rotoma, 9.5 ky $7.76 \pm 0.17\text{‰}$ 2SD, and Kaharoa, 0.7 ky, $7.38 \pm 0.27\text{‰}$ 2SD), one from each of the inter-caldera volcanic complexes. With the exception of Haparangi, data imply source uniformity over time, with an overall balance between mantle and crustal inputs. Future work includes additional quartz $\delta^{18}\text{O}$ analyses of other units, and extending the work to other isotopic systems in different minerals (i.e. Sr and Pb in plagioclase).

QUANTIFYING MAGMA STORAGE TIMESCALES AND THERMAL HISTORIES FOR THE ~25 KA ORUANUI AND 1.8 KA TAUPO ERUPTIONS OF THE TAUPO VOLCANIC CENTER, NEW ZEALAND

Schlieder T., K.M. Cooper, A.J.R. Kent, D. Gravely, C. Deering

The timescales and thermal conditions involved in the generation of silicic magmas within the crust is of fundamental importance to volcanology, and yet constraints on these factors remain elusive. We use new ^{238}U - ^{230}Th ages and diffusion timescales from the ~25ka Oruanui and 1.8 ka Taupo eruptions from the Taupo Volcanic Center (TVC), New Zealand to quantify pre-eruptive thermal conditions of magma storage within the TVC magma reservoir. Preliminary major phase ^{238}U - ^{230}Th ages are within error of eruption for both Oruanui and Taupo, in contrast with zircon interior ages from Oruanui which extend to >100 ka. This discordance indicates that plagioclase grew shortly before eruption, whereas zircons were extracted from a longer-lived portion of the system. Sr-in-plagioclase diffusion timescales indicate magmas spent 750°C before eruption. The similar magnitude of plagioclase ^{238}U - ^{230}Th ages and Sr diffusion timescales, coupled with protracted zircon ages, suggests TVC rhyolites are extracted from a long-lived portion of the reservoir and stored as >750°C mobile magmas for short timescales (10 kyrs) as cool (<750°C) crystalline mush prior to rapid remobilization and eruption.

UPPER MANTLE HETEROGENEITY: DEPLETED SOURCE SIGNATURE PRESERVED IN MELT INCLUSIONS AT COAXIAL SEGMENT OF THE JUAN DE FUCA RIDGE

Schwartz D., V.D. Wanless

We assess the origins of a highly depleted mantle component, which is sampled along the Juan de Fuca Ridge (JdFR) that has been previously observed in basalts and melt inclusions on and off-axis of Coaxial Segment. To better determine the endmember composition of this source at Coaxial, we have analyzed olivine-hosted melt inclusions (MIs; N=113) and host glasses (N=7) for major, trace and volatile element contents, which we compare with new and existing data from Vance and Cleft segments of the JdFR. Of the three segments, Coaxial has the most diverse range of MI compositions, which we divide into two categories based on major and trace element systematics: NMORB ($\text{La/Sm} > 0.5$ and $\text{K}_2\text{O/TiO}_2 > 0.05$; N=68) and DMORB ($\text{La/Sm} \leq 0.5$ and $\text{K}_2\text{O/TiO}_2 \leq 0.05$; N=45). NMORB inclusions closely resemble those measured on Cleft and Vance. DMORB inclusions are characterized by higher mean FeO/MgO (0.93) and $\text{H}_2\text{O/Ce}$ (0.076) compared to NMORB ($\text{FeO/MgO} = 1.1$ and $\text{H}_2\text{O/Ce} = 0.032$). Lower average FeO/MgO of the DMORB MIs support early, likely deep, entrapment compared to the NMORB inclusions. While DMORB compositions have been explained by high extents of melting of a normal mantle component, we show that coupled depletion of La/Sm (or $\text{K}_2\text{O/TiO}_2$) and enrichment of $\text{H}_2\text{O/Ce}$ (or $\text{H}_2\text{O/K}_2\text{O}$) in the Coaxial MIs can be modeled as mixing between DMM melts with melts derived from a more depleted source, which we model as DMM previously depleted by 2% melt extraction with water diffusively reset.

A FOCUS ON MELT FOCUSING

Sim S.J., M. Spiegelman, C. Wilson, D. Stegman

Magmatism at mid-ocean ridges generates new oceanic crust and accounts for 90% of global volcanism. The oceanic crust is emplaced in a narrow neo-volcanic region (e.g. Macdonald (1982); Carbotte et al. (2016)), whereas basaltic melt is generated in a wide region beneath mid-ocean ridges as suggested by a few geophysical surveys (Forsyth et al., 1998b; Key et al., 2013). A number of focusing mechanisms have been proposed such as ridge suction (Spiegelman and McKenzie, 1987) and decompaction layers (Sparks and Parmentier, 1991). The purpose of this work is to demonstrate and highlight melt focusing mechanisms present in melt in the mantle two phase formulation with viscous deformation. We present results from a suite of two-phase models applied to the mid-ocean ridges, varying half spreading rate ($U_0 = 2, 4, 8$ cm/yr) and background permeability ($K_0 = 4 \times 10^{-7}, 10^{-9}$ m²) using a new openly available model, Melt in the Mantle beneath Mid-ocean ridges (M3LT) models. M3LT models are built using TerraFERMA, the Transparent Finite Element Rapid Model Assembler (Wilson et al., 2017), which is flexible and therefore can be extended relatively easily. M3LT models solve for the magma migration equations (McKenzie, 1984) with thermal evolution, non-linear rheology and melting that depends on pressure and temperature. The M3LT models suggest that models with similar melting patterns can have significant differences in melt transport patterns due to changes in background permeability, K_0 . The permeability of the solid mantle determines melt transport, porosity and therefore compaction length, which is the length scale at which the solid mantle viscously respond to move melt around. As a form of validation, the predicted oceanic crustal thicknesses versus spreading rates from the M3LT model fit reasonably amongst the observations from geophysical surveys. Three distinct melt focusing mechanisms are recognized in the M3LT models: 1) Melting pressure focusing, 2) Decompaction layers and 3) Ridge suction, which is small and only affects the area around the ridge axis. As a natural consequence of the two phase flow formulation with viscous deformation, the manifestation of these mechanisms depends largely on the rheological parameterization. Melting pressure focusing is simply due to a balance of compaction pressure with melting rate scaled by the bulk viscosity and compaction length at quasi-steady state. Melting is determined mainly by the solid mantle upwelling, which is fairly well constrained. In the M3LT models presented here, the background permeability determines the dominant melt focusing mechanisms since it controls the compaction length. Analyzing the proportion of melt flux focused by either mechanism, we determine that melting pressure focusing is dominant for high permeability models whereas decompaction layer is dominant for low permeability model. From the melt flux analyses, there is also a secondary trend of melting pressure focusing decreasing and decompaction layer increasing with spreading rate independent of permeability, which could be due to the decreasing “mobility” with increasing spreading rate. Geophysical observations of the amount of partial melt present beneath mid-ocean ridges is compared with the M3LT models, potentially giving us constraints on background permeability. The agreement and disagreement of the locations of high melt regions between the M3LT models and geophysical observations hint at the extend of this melting pressure focusing, given that it focuses melt before melt can reach the decompaction layers. Last but not least, we infer the geochemical signatures expected from the M3LT models based on degree and depth of melting.

RUPTURING PARADIGMS OF CONTINENTAL RIFT MAGMATISM: A CHEMO-SPATIAL ANALYSIS OF RIFT MAGMAS

Steiner A., T. Rooney, E. Micuda

Volcanic episodes associated with continental rifting are often considered to be small in volume, manifesting as monogenetic cinder cones and limited flows that comprise stratovolcanoes. This simplified model of rift magmatism is, however, inadequate in describing volcanic activity within the East African Rift (EAR). Here, periodic, voluminous, and compositionally homogenous eruptions occur throughout the temporal development of the rift. Constraining the origin and relationship of these events to rifting process provides insights into the episodic nature of the rift magmatism. The Pliocene Gombe Group basalts, a widespread and homogenous volcanic episode, has been identified east and west of lake Turkana through southern Ethiopia. This study applies trace element geochemistry and spatial analysis of temporally associated mafic volcanics to elucidate the total extent and origin Gombe group. The trace element distributions are consistent with melts derived from a peridotite located above the garnet-spinel transition zone. Spatial and geochemical analysis of contemporaneous mafic volcanics expand the Gombe Group basalts to the South and East. Given the narrow age and homogenous composition, the Gombe group magmas likely formed from a single regional-scale event accessing a shallow melting column coincident with rifting from Southern Ethiopian through eastern Turkana and into the Kenya rift.

A GLOBAL VIEW ON ARC-TRENCH CONNECTIVITY AND ANDESITE PETROGENESIS

Straub S.

The magnitude of the recycled arc flux is clearly linked to andesite petrogenesis, and thus to the enduring debate on whether andesite magmas are slab-mantle mixtures or whether they evolve from basaltic parental melts by AFC-type processes in the upper plate crust. Here I address this question through a evaluation of global arc magma compositions from 32 arc segments that comprise n=12,856 major and trace element data and n=5,331 Sr-Nd-Pb-Hf isotope ratios. These data show that there is no global correlation of arc SiO₂ with crustal thickness, nor a correlation of Sr-Nd-Pb-Hf isotope ratios with arc SiO₂, Mg# or MgO and other parameters predicted by models of andesite formation by upper plate crustal contamination. While the range of global arc Sr-Nd-Pb-Hf isotope ratios compares to that of MORB and upper continental crust, the composition of individual arc segments is controlled by source components specific to given arc trench systems. The latter observation is consistent with andesite evolution by closed-system fractional crystallization, yet such process is inconsistent with the pervasive evidence of melt mixing which characterize arc magmas on microcopic and macrocopic scales. Alternatively, the data can be reconciled with models where a range of recycled crustal components (fluids, partial melts, slab diapirs and plumes) are transferred to the mantle wedge where they variably mix and react with peridotite and eventually give rise to a broader spectrum of mafic and evolved melts that may pass the upper plate crust largely unchanged.

EVOLUTION OF TRANSCRUSTAL DISTILLATION COLUMNS: EVIDENCE FROM ANDESITES OF THE TAUPO VOLCANIC ZONE

Svoboda C., T. Rooney, C. Deering, G. Girard

Synthesis of field work, numerical simulations, and geophysical observations indicates that in many magmatic systems, mantle-derived magmas evolve within complexes of dikes and sills. These complexes, recently termed "Transcrustal Distillation Columns (TDCs)", are important in explaining the diversity of lavas in arcs. The incipient stages of such columns are difficult to probe. The stratovolcano Ruapehu and associated vents in the Taupo Volcanic Zone (New Zealand) provide an opportunity to examine the evolution of such TDCs. Magnesian andesites from Ohakune contain primitive olivine and pyroxene crystals but are devoid of plagioclase, suggesting that these andesites represent incipient phases of TDCs. Fe-Mg crystal/melt disequilibrium suggests that the crystal cargo of Ohakune andesites are scavenged from the deepest levels of the magmatic system, just prior to eruption. By examining the multiple vents in this volcanic center, we reveal an evolutionary pathway for TDCs. The column is initially dominated by crystallization of mafic phases and restricted to the lower crust. With sustained magmatic intrusion, the TDC develops into the upper crust; plagioclase begins crystallizing, and exchange of material between the upper and lower zones becomes restricted. This evolutionary model is likely globally applicable to studies of the magmatic systems in rifting and subducting margins.

LITHOSPHERIC THICKNESS OF VOLCANIC RIFTING MARGINS: CONSTRAINTS FROM SEAWARD DIPPING REFLECTORS

Tian X., W.R. Buck

Seaward Dipping Reflectors (SDRs) are large piles of seaward-thickening volcanic wedges imaged seismically along most rifted continental margins. Despite their global ubiquity, it is still debated whether the primary cause of SDR formation is tectonic faulting or magmatic loading. To study how SDRs might form we developed the first two-dimensional thermo-mechanical model that can account for both tectonics and magmatism development of SDRs during rifting. We focus here on the magmatic loading mechanism and show that the shape of SDRs may provide unprecedented constraints on lithospheric strength at volcanic rifting margins. For mapping SDRs geometries to lithospheric strength, a sequence of model lithospheric rheologies are treated, ranging from analytic thin elastic plates to numerical thick elasto-visco-plastic crust and mantle layers with temperature and stress dependent viscosity. We then analyzed multi-channel seismic depth-converted images of SDRs from Vøring and Argentinian rifted margins in terms of geometric parameters that can be compared to our model results. This results in estimates for the lithospheric thickness during rifting at the two margins of 3.5 and 5.9 km. The plate thickness correlates inversely with mantle potential temperature at these margins during rifting, as estimated by independent studies.

A MODEL FOR THE FIRST ORDER CONTROLS ON VOLCANIC REPOSE TIME

Till C., A. Kent, K. Cooper

The first order tectonic and mantle processes that produce volcanoes are relatively well understood. However, the more specific processes dictating "volcano personality" i.e. the overall range of erupted compositions, the eruptive styles, and repose interval of particular volcanoes and their variations within a given tectonic setting are relatively poorly known. Passarelli and Brodsky (2012, GJI) demonstrate that on a global scale, volcanic repose time and silica content are highly correlated, with more mafic systems having shorter repose times relative to silicic ones. A recent paper by Till et al. (in press, Nature Comm.) also demonstrates a relationship between erupted compositions and volumes, and the mantle-derived magmatic flux into the base of the crust for the Cascades arc, which varies by >100% along strike. Here we put these concepts together to test the hypothesis that the flux of mantle-derived magmas produces an important control on variations in the repose time between individual volcanoes within a given tectonic environment. For example within the Cascades arc, we find that the large arc volcanoes exhibit correlations between mantle magmatic flux and repose time. In addition, the southern portion of the arc, which has at least twice the flux of mantle-derived magmas into the crust relative to the northern arc, appears to require a higher mantle magmatic flux per a given repose time. This hypothesis can be further tested by compiling detailed information for along strike variations in volcanic repose time and calculation of mantle basalt flux for the same systems.

MATERIAL TRANSPORT IN THE MANTLE THROUGH 4-D GEODYNAMICAL MODELS OF MID-OCEAN RIDGES

van Dam L., C. Kincaid

Lateral migration of mid-ocean ridge spreading centers is a well-documented phenomenon leading to asymmetric melt production and the surficial expressions thereof. This form of plate motion is difficult to incorporate into geodynamical models, and consequently, current estimates of time-dependent flow, material transport, and melting beneath ridges are lacking. To address this, we have designed and built an innovative research apparatus that allows for precise and repeatable simulations of both spreading and migration. The apparatus is suspended above a reservoir of viscous glucose syrup, a scaled analogue for the upper mantle. We image plate-driven flow in the syrup with high-resolution digital cameras and use particle image velocimetry to obtain quantitative information about the flow. Results show that in the presence of a migrating ridge, mantle material exhibits a significant degree of lateral transport, particularly between ridge segments and towards the melt triangle. Parcels of material do not necessarily move along fixed streamlines, rather, they can be perturbed upwards and left behind. These results emphasize that observations of seismic anisotropy should be interpreted in light of intricate flow pathlines and that melt transport models should consider different paths for melt relative to the solid matrix.

SEISMIC CONSTRAINTS ON SUBDUCTED HYDROUS MINERALS IN THE TONGA SLAB

Wei S.S.

Earth's deep water cycle is mainly controlled by hydrous minerals subducted within slabs, such as lawsonite in the subducted crust and serpentine in the slab uppermost mantle. The distribution of these hydrous minerals has been previously investigated with seismic imaging, petrological/mineralogical experiments, and geodynamic modeling. These efforts were usually focused on subduction zones in Northeast Asia, North America and South America, with thermal states ranging from warm (Cascadia and Nazca) to relatively cold (Japan and Alaska). The Tonga slab, at least 200°C colder than other slabs at depths >150 km [Syracuse et al., 2010], provides an extreme case to study subducted hydrous minerals. Particularly, Wei et al. [2017] discovered a seismic belt in Tonga at depths of 160-280 km, potentially indicating antigorite dehydration down to 280 km, but lacking of direct evidence. I analyze seismic waves of local earthquakes converted at the Tonga slab surface and recorded by local stations to image high-resolution structures of the Tonga slab interior at depths of 50-300 km. The preliminary results provide insights into the distribution of the subducted hydrous minerals in this coldest slab.

MARIANA SUBDUCTION ZONE WATER INPUT ESTIMATED FROM BROADBAND OCEAN-BOTTOM SEISMIC DATA

Cai C., D. Wiens (presenter), W. Shen, M. Eimer

Previous estimates of the water cycle at subduction zones show large uncertainty in the amount of water subducted deeper than 100 km. A major problem in these calculations is that the initial water content of the subducting uppermost mantle is poorly constrained. We present new seismic images of the crust and uppermost mantle around the central Mariana Trench derived from Rayleigh wave analysis of ocean bottom seismic data, showing that slow velocities resulting from mantle hydration extend 24 ± 5 km beneath the Moho. Combined with estimates of subducting crustal water, these results indicate that at least 4.3 ± 0.8 times more water subducts than previously calculated for this region. If other old, cold subducting slabs contain correspondingly thick layers of hydrous mantle, as suggested by the similarity of incoming plate faulting, estimates of the global water flux into the sub-arc mantle must be increased by about a factor of three over previous estimates. Since a long-term net influx of water to the deep interior is inconsistent with the geological record, it is likely that estimates of water expelled at volcanic arcs and back arc basins also must be revised upward.

CLINOPYROXENE TRACE ELEMENT CHEMISTRY AS A PROXY FOR MAGMA COMPOSITIONAL VARIATIONS IN THE IZU BONIN REAR ARC OVER THE LAST 14 MILLION YEARS

Wurth K., S. DeBari

The Izu-Bonin intraoceanic arc in the western Pacific exhibits an asymmetry in geochemical signatures between the arc front and the rear arc (Hochstaedter et al. 2001, Tollstrup et al. 2010). The arc front displays a light rare earth element (LREE) depleted signature relative to heavy REE while the rear arc demonstrates a LREE enriched signature. The International Ocean Discovery Program (IODP) Expedition 350 drilled a volcanoclastic core representing 0-14 Ma. One of the many goals of Expedition 350 was to determine if the LREE enriched signature was a characteristic of the rear arc throughout the arc's history or if it was a recent development (Busby et al. 2017). The purpose of this study is to test a method of calculating liquid compositions from clinopyroxene grains using distribution coefficients. If the method is confirmed, the calculated melt chemistries will be used to evaluate competing hypotheses regarding rear arc formation. Major and trace element chemistry of clinopyroxene grains has been evaluated via SEM and LA-ICP-MS at Western Washington University. Preliminary REE plots suggest some change in melt chemistry throughout the core, however analysis of the data and confirmation of the methodology is still in progress.

SEISMIC IMAGING OF SLAB SEGMENTATION AND ITS CORRELATION WITH VOLCANO DISTRIBUTION ALONG THE ALEUTIAN-ALASKA SUBDUCTION ZONE

Yang X., H. Gao

The along-strike variation of volcanic activities has been observed at many subduction zones. However, direct structural constraints on how volcano distribution is influenced by slab geometry and mantle wedge properties are limited. Using full-wave ambient noise tomography, we constructed a high-resolution shear-wave velocity model for the Aleutian-Alaska subduction zone. The model reveals multiple slab segments with varied mantle wedge velocities, correlating with the distribution of active volcanoes and a volcanic gap. The distinct low-velocity mantle forearc atop the Pacific slab implies a wet mantle wedge associated with the volcanic arc. Contrastingly, the mantle wedge beneath the Denali volcanic gap, with much higher velocities, reflects a dry environment. The tomographic results provide evidence for the control of mantle wedge hydration states on magmatism at subduction zones.



PennState

GeoPRISMS Office, The Pennsylvania State University
503 Deike Building | University Park, PA 16802-2714

2019 GeoPRISMS Synthesis and Integration Theoretical & Experimental Institute
February 27 - March 1, 2019
Poster Abstract Volume

